Coastal fog at the North Sea: Is a sea breeze circulation required for its initiation, maintenance and dissipation?

by

C.L. Vanwersch

1028079

MSc Thesis

Meteorology and air quality

MAQ-80836

Wageningen University & Research

Supervised by Dr. Ir. G. Steeneveld

Date: 19 April 2024

Contents

Abstract 3
List of abbreviations 3
1. Introduction 4
1.1. Background 4
1.2. Advection fog 4
1.3. Coastal fog 4
1.4. Sea breeze circulation 5
1.5. Problem and research analysis 6
1.6. Research questions 6
1.7. Outline 6
2 Methods and data 7
2.1. Case selection 7
2.2. WRF configuration 7
2.3. Data sources and validation 9
2.4. Experiments 9
2.5. Analysis 11
3 Results 12
3.1. Validation of WRF 12
3.2. Sensitivity experiments 14
3.2.1. Reference run 20
3.2.1. Equal Temperature 20
3.2.2. SST up and SST down 20
3.2.4. Urbanisation and De-urbanisation 21
3.2.5. Correlation 21
4 Discussion 22
4.1. Validity of Results 22
4.2. Formation of Coastal Fog 22
4.3 Limitations 23
4.5. Future Research Directions 23
5 Conclusion 24
Acknowledgements 25
References 26
6 Appendix 28

Abstract

Coastal fog at the Dutch coast has proven to be a complex phenomenon that puzzles meteorologists and is hard to forecast. The fog often occurs unexpectedly, resulting in hazardous situations for shipping and aviation, not to mention a disappointment for beach visitors who stumble upon the cold and moist wall of fog. It is therefore important to increase the understanding of meteorological processes that initiate coastal fog. This study aims to answer whether and how coastal fog is able to occur without a sea breeze circulation and which meteorological factors enhance or exert the initiation of coastal fog. A coastal fog case at the Dutch coast on the 20th of May 2018 was replicated with the Weather and Research Forecasting model. Sensitivity experiments with a converted SST and a converted land use were performed. In conclusion, a higher land-sea temperature gradient induces the initiation of coastal fog. An urbanized coastline enhances marine fog formation but obstructs the fog to reach the shore due to an increased turbulence. Coastal fog may manifest without the presence of a sea breeze circulation. Nonetheless, the presence of such circulation appears to enhance the initiation of coastal fog, explaining their frequent simultaneous occurrence. Further research is needed to investigate the correlation between urban areas and land-sea temperature gradient with respect to coastal fog formation, as well as the interdependence of coastal fog on sea breeze circulation.

List of abbreviations

ARW	Advanced research WRF
CIBL	The convective internal boundary layer
ECMWF	European Centre for Medium-Range Weather Forecasts
HFX	Sensible heat flux
KHB	Kelvin-Helmholtz billows
LST	Land surface temperature
LWP	Liquid water path
P	Pressure
QCLOUD	Cloud water mixing ratio
RH2	2 meter relative humidity
SBC	Sea breeze circulation
SBF	Sea breeze front
SBH	Sea breeze head
SST	Sea surface temperature
T2	2-meter Temperature
WRF	Weather and Research Forecasting

1. Introduction

1.1. Background

Earth accommodates a dynamical and complex ecosystem in which the oceans play a crucial role in regulating climate and atmospheric processes (Eckart, 2013). Multiple atmospheric phenomena occur in this maritime scenery, which challenge and stimulate meteorologists for further research. One of these intriguing appearances is 'coastal fog'; sea fog occurring in coastal regions which extents approximately up to the coastline where it dissipates into clear air, leaving a vertical wall of mist stretching over the sea to see for lucky spectators.

Sea fog is closely associated with the interactions between marine environment, the atmosphere, and the coastal land. Meteorological factors such as wind, air temperature, relative humidity and turbulence have an important role in shaping the manifestation of coastal fog (Lee et al., 2021). The study of coastal fog not only enhances our comprehension of these intricate atmospheric processes, but also sheds light on the broader implications for local climate and weather conditions. Moreover, coastal fog introduces noteworthy consequences to the local climate by influencing the energy balance, subsequently altering the temperature and precipitation patterns. The presence of sea fog/coastal fog has a significant impact on both human activities and the environment. Most accidents happening at sea came about under foggy conditions, as fog significantly decreases the visibility, hindering navigation and therefore practicing its influence on shipping and aviation. Coastal fog remains a significant challenge for meteorologists due to its complexity and incomplete understanding.

1.2. Advection fog

Fog consists of water droplets or ice crystals suspended near the Earth's surface, causing the near-surface visibility to drop below 1km (Myers, 1968; Fernando et al., 2021). It can be recognized as a cloud in contact with the surface, which can be formed in different ways. Radiation fog is formed overnight, as the surface cools down by sending out longwave radiation without receiving shortwave radiation from the sun (Roach et al., 1976). The (emitting) surface gets colder than the (absorbing) air, resulting in the formation of fog. After sunrise, the shortwave radiation heats the surface again, resulting in dissipation of the fog (Fernando et al., 2021). Advection fog arises when either cold air is advected over a much warmer water body, or warm air is advected over a much colder water body (Nakanishi & Niino, 2006). In case of a warm water body, water vapor evaporates from the water into the air, causing the air to be saturated quickly. The warm moist air is advected and ends up in colder air, where the dew point temperature is reached and fog is formed. This phenomenon mostly happens over water bodies like lakes and rivers in autumn and early winter, as cold air is advected over the warmer water, which cools down slower (Fernando et al., 2021). When moist warm air is advected over cold water, the air near the surface cools down causing it to reach the dew point temperature resulting in fog (KNMI, 2018; Wolters et al., 2011). A simple overview of advection fog is shown in figure 1.1. Conditions favourable for the formation of this advection fog near the coast are typically provided in spring and early summer, as the water of marine environments does not warm up as quickly as the continental environment.

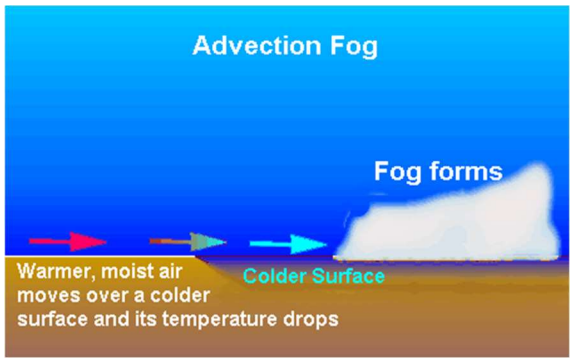

Figure 1.1: Mechanism of advection fog (Hoofdstuk 7. Zicht, mist en dauw, z.d.)

1.3. Coastal fog

When the cold sea surface and the warm moist terrestrial air encounter, advection fog is initiated over the sea surface when the dew point temperature is reached. In case the fog is then transported landward, coastal fog (Dutch; 'Zeevlam') occurs. Typically, temperatures over land in May and June are summery,

causing the temperature of the air parcel to exceed the dew point temperature once the shoreline is overtaken, resulting in dissipation of the fog. Wind direction and magnitude are crucial factors on which the occurrence of coastal fog depends (KNMI, 2018). A seaward wind direction will prevent the sea fog from reaching the shoreline, whilst a landward wind direction will transport the fog to the shoreline. A very strong wind, however, can also result in dissipation of the fog due to turbulence. Furthermore, thunderstorms moving from land to sea can also influence the fog and are an important factor in the maintenance of the phenomenon (KNMI, 2018). Briefly, the occurrence of coastal fog requires very specific conditions. The phenomenon is observed a few times a year at the Dutch coast (Floor, 2013).

Summery weather occurs simultaneously with rapid heating of the land surface and thus upward movement of warm air. As a result, marine air is advected to compensate the air flow, inducing a sea breeze circulation (SBC); cold marine air is advected over land and warm terrestrial air is advected over sea. Intuitively, the initiation of coastal fog is stimulated by an SBC, as the circulation provides the perfect conditions for the warm moist air to reach the cold sea surface. Therefore, meteorologists often associate Coastal fog with SBC. However, Kees Floor (2013) describes multiple cases for which coastal fog occurs without an SBC, raising questions about the correlation between SBC and coastal fog.

1.4. Sea breeze circulation

An SBC is a local circulation that occurs in coastal regions worldwide (Masselink, 1998; Miller et al., 2003). It can provide alleviation from hot oppressive weather, trigger thunderstorms, or bring moisture enhancing the formation of fog (Camberlin & Planchon, 1997; Silva Dias & Jaschke Machado, 1997). SBC's are initiated by differential heating of air over land and air over sea. Tijm et al., (2003), state that a sea breeze generally commences as a light shoreward surface wind, perpendicular to the coast. The sea breeze system consists of multiple components, shown schematically in figure 1.2:

- Sea breeze circulation (SBC) embodies a vertically rotating mesoscale cell near the Earth's surface, flowing shoreward. It can be recognized by rising air currents over land and descending air currents several kilometres seaward.
- Sea breeze gravity (SBG) current is the cool and moist marine air flowing landward close to the sea surface.
- Sea breeze front (SBF) describes the landward edge of the SBC and the SBG. The SBF typically provides sharp changes in temperature, moisture and wind. The development of fair-weather cumulus clouds (Cu) often indicate an approaching SBF.
- Immediately behind the SBF, the sea breeze head (SBH) is located. Updrafts in both continental and marine air masses enhance the SBH which is approximately double the height of the following flow behind the flow behind the SBH.
- Kelvin-Helmholtz billows (KHB's) are small waves, located between the SBH and the shoreline. These are formed along the upper boundary of the SBG when there is low static stability (midday) due to friction with the warmer air mass flowing in the opposite direction directly above.
- The convective internal boundary layer (CIBL) comprises an unstable region of marine air mass starting at the coast and growing land inwards. (Miller et al., 2003)

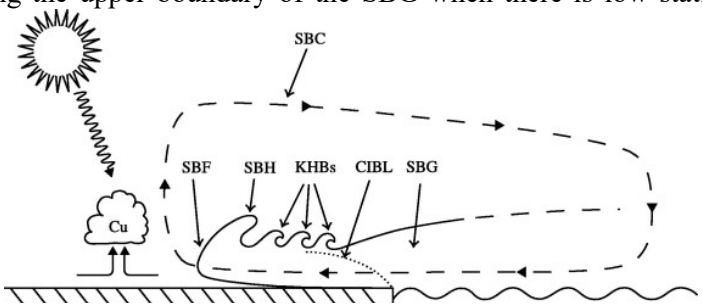

Figure 1.2 Schematic overview of the sea breeze system and its components (Miller et al., 2003)

Similar to coastal fog, SBC at the Dutch coast occurs every year in spring and summer. As it is induced by summery weather, SBC is observed frequently in this period of the year. The rising air

above land is obstructed when it reaches the planetary boundary layer, typically around 1.5km in the time of year in the Netherlands. After which it is advected horizontally towards the sea.

Throughout this report, both terms sea fog and coastal fog have been and will be used frequently. Let there be no doubt, that both terms refer to the same advection fog, where sea fog refers to an event were the fog does not reach the coastline and coastal fog refers to an event when the fog does indeed reach up until or beyond the coastline.

1.5. Problem and research analysis

Coastal fog is very unpredictable and hard to simulate due to its complexity. A comprehensive research that integrates dynamics, microphysics and thermodynamics related to coastal fog formation, persistence, and dissipation is needed to touch upon the understanding of coastal fog (Fernando et al., 2021). Especially evaluation and improvement of microphysical parameterizations related to fog combined with three dimensional wind directions can improve the evaluation of fog intensity (Gultepe et al., 2021). This research will aim to contribute to the aforementioned challenges to improve the forecasting of coastal fog at the Dutch coast. The main goal of this study is to analyse the dependence of coastal fog on SBC and find other factors that exert an influence on its initiation, maintenance and dissipation. The Weather Research and Forecasting model WRF (Skamarock et al., 2019) will be used to do multiple sensitivity experiments on a coastal fog case that occurred the 20th of May 2018 (Figure 2.1), to identify previously mentioned conditions and to provide elaborate answers to the following research questions.

1.6. Research questions

1. Through which mechanism could the formation of coastal fog be possible in the absence of a sea breeze circulation?
2. Which meteorological variables and geographical characteristics exert the most significant influence on the initiation of coastal fog?

1.7. Outline

The remainder of the report is organized as follows. Chapter 2 discusses the methodology, starting with the case selection. Data sources and configuration of WRF are discussed extensively after which the different sensitivity experiments are introduced. Chapter 3 thoroughly shows the most important results which will be discussed in Chapter 4 and concluded on in Chapter 5.

2 Methods and data

2.1. Case selection

The coastal fog case shown in Figure 2.1 was chosen carefully according to some prerequisites. First of all, a clear satellite picture of the event had to be available. Secondly, data from observational meteorological weather stations had to be satisfactory. Lastly, ECMWF data that were used as boundary conditions needed to be available. The latter two will be discussed further in the following section.

Figure 2.1: Satellite image of a coastal fog case 20th May 2018 13:00, 15:00 UTC (KNMI, 2018)

2.2. WRF configuration

The fully compressible, non-hydrostatic Advanced Research WRF (ARW) version 4.3 model was used to conduct this research (Skamarock et al., 2019). The WRF model can simulate atmospheric simulations over a certain time period which will first be used to validate the model. After configuration of the model domains, ingestion of the input and preparation of the initial conditions, the hindcast model can be run. The initial and boundary conditions are retrieved from ECMWF (European Centre for Medium-range Weather Forecasts). After every six hours, the model will be forced by ECMWF operational analysis at 0.11 degree at the lateral boundaries.

The integration time will amount to a length of 2 days and 12 hours. Starting the 19th of May 00:00 UTC 2018 until the 21th of May 12:00 UTC 2018. This includes one day of spin up before the coastal fog occurred to see how the synoptical situation develops to create the conditions that favour the formation of coastal fog (Shao et al., 2023). A spin-off period of 12 hours is also included to see how long the fog holds and analyse how it resolves again.

Parameterization schemes play an important role in resolving sub-grid processes, which cannot be resolved by the numerical grid resolution in WRF and help decreasing the computational time of the model and consequently the costs of the simulation. They are mathematical representations or algorithms that try to capture the effect of these sub-grid processes on the state variables like temperature, wind, humidity and cloud formation (Powers et al., 2017). There is a large spectrum of parameterization schemes for different processes that can be used in WRF. According to Yang et al. (2019), the formation of sea fog is the most sensitive for the Planetary boundary layer (PBL) parameterization scheme. Both the Yonsei university (YSU: Hong, 2010) and the Mellor-Yamada-Nakanishi-Niino (MYNN: Nakanishi & Niino, 2009) are two of the more skilled PBL parameterization schemes, of which the YSU scheme

was found to perform better over the flat terrain of the Netherlands with more accurate timing of onset, more widespread fog area and higher liquid water content (Steeneveld et al., 2015, Yang et al., 2019). Therefore, the YSU scheme will be used as parameterization for the PBL. Other parameterization schemes are listed in Table 2.2

Table 2.1: Overview of the used parameterization schemes.

MODEL PHYSICS	PARAMETERIZATION SCHEME
PLANETARY BOUNDARY LAYER	MYNN (Olson et al., 2019)
MICROPHYSICS	Lin (Lin et al., 1983)
CUMULUS SCHEME	Kain-Fritsch (Kain, 2004)
LONG/SHORTWAVE RADIATION	RRTMG (Rapid radiative transfer model for general circulation models)
LAND SURFACE	NOAH (Srivastava et al., 2015)

The simulation contains two nested domains as shown in Figure 2.2. Domain 1 will be used to follow the synoptic situation towards the case of coastal fog. It includes the entire North Sea and part of the Atlantic to capture the processes happening above these large water bodies and to analyse the influence of the jet stream. Domain 2 will be used to closely look at the processes taking place concerning the fog initiation, maintenance and dissipation. Both domains will have 44 eta (vertical) levels with the highest level at 10km in order to capture both vertically and horizontally the complex microphysical and thermodynamic processes which are especially important in fog formation. It is aimed to apprehend the processes happening near the surface so 15 of the eta levels are in the lowest part of the atmosphere beneath 1 km with the lowest level at the surface, a setup that was also used by Fernando et al., (2021). A relatively higher resolution in the bottom layer is important to capture. A higher vertical resolution would result in more accurate results, but taking into account the computational time and costs, it has been decided that 44 eta levels will provide a sufficient accuracy to answer the research questions in section 1.6. Domains one and two will have a resolution of $3km^2$ and $1km^2$ respectively, which was also used by Lee et al., (2021) to capture sea fog at the Yellow Sea at the coast of China. Domain one is processed with a time step of 20 seconds and domain two, being three times as frequent, is processed every 6.7 seconds. Output is created after every six hours for domain 1 and after every hour for domain one.

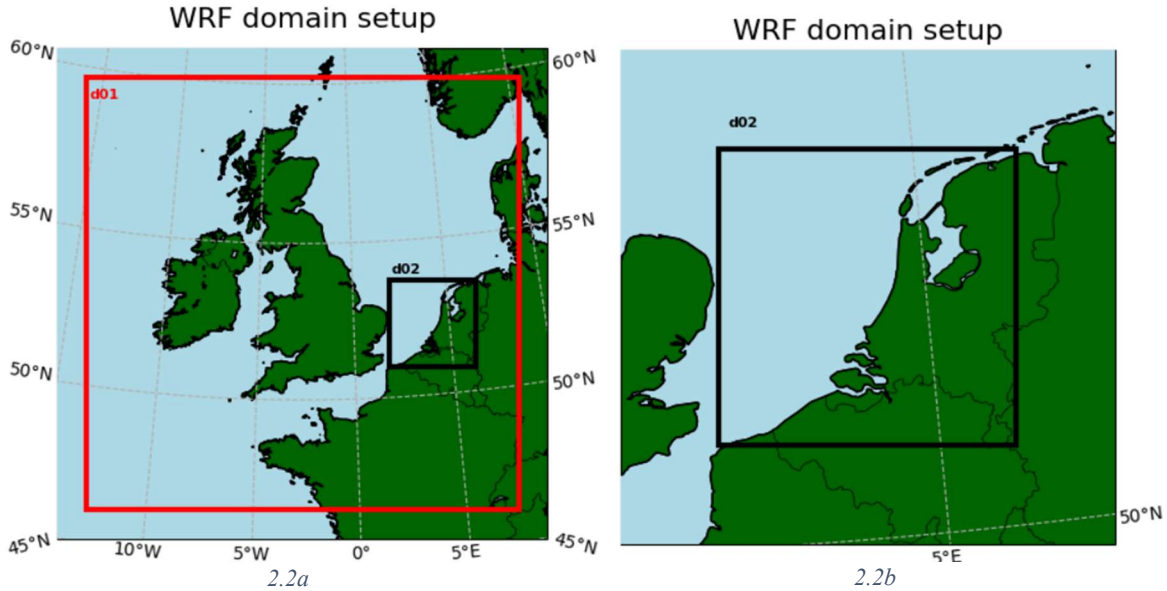

2.2a *2.2b*

Figure 2.2: Spatial representation of domain one and two

2.3. Data sources and validation

Hourly observational data retrieved from KNMI (Koninklijk Nederlands Meteorologisch Instituut) will be used to validate the atmospheric simulation by WRF. The variables that will be used for validation are visibility (2m), relative humidity (2m), temperature (2m), dew point temperature (2m), mean sea level pressure, wind speed (10m), angle of wind and cloud liquid water content. The KNMI provides these data from several meteorological weather stations on the North Sea, shown in Figure 3.1a. The following three meteorological weather stations will be used to validate the WRF-simulation; Hoorn-A, P11-B and Euro Platform. The position of the weather stations with respect to the location of the fog can be compared when combining Figure 2.1a and Figure 2.1b. Unfortunately, the other meteorological stations shown in Figure 2.1a could not be added as validation points as the required data was either not available for the needed dates or did not contain the required variables.

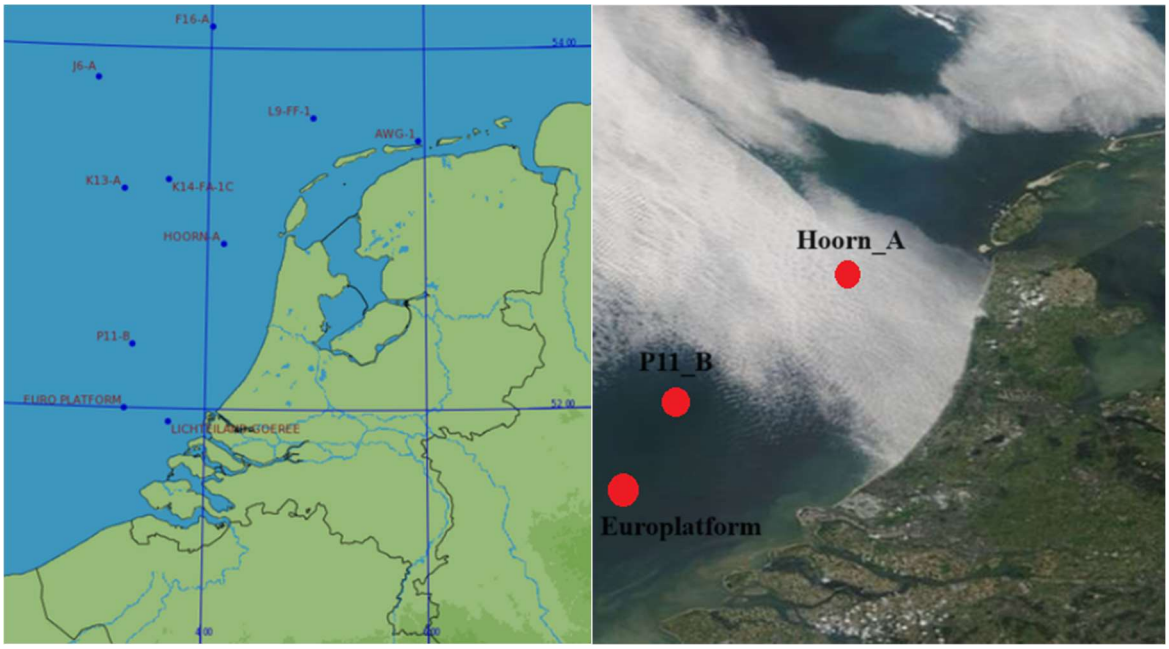

Figure 2.1: a; Overview of meteorological weather stations on the North Sea (KNMI, 2018). b; Coastal fog case on the 20th of May 2018 (KNMI, 2018).

To validate the WRF simulation, both the root mean squared error and mean absolute error were calculated for the 2-m relative humidity, the 2-m temperature, and the sea surface pressure. Due to abrupt alterations in weather conditions as a result of the fog, a very small difference in timing of the fog can result in large changes in the metrics, especially for the relative humidity, temperature and visibility. Furthermore, a slight dislocation of the fog might result in completely different results compared to the observed data for one of the meteorological weather stations. In case of poor metrics that can however be explained by the timing and location of the fog, the model can be validated either way, whilst taking in to account that the simulated WRF-model is slightly off.

2.4. Experiments

Multiple sensitivity experiments were performed with WRF in order to get answers to the research questions. The experiments are listed in Table 2.3 and expected results are described in Table 2.4. An important detail is that the described adjustments to the WRF model have been made with respect to the reference run. For instance, the total adjustment of the SST for experiment 3 is an increase of 2.4˚C compared to the SST retrieved from the ECMWF. Similarly, the total decrease of SST for experiment 4 is 3.6˚C.

For the land use experiments (5 and 6) the pink area arcaded in Figure 2.3 has been adjusted. For the urbanization experiment, the adjusted area is turned into one large city. For the de-urbanization experiment, the area is turned into a cropland/natural vegetation mosaic.

Table 2.2: Overview of the sensitivity experiments performed with WRF

EXPERIMENT	SENSITIVITY EXPERIMENT	MODEL	PARAMETER ADJUSTMENT
1	Reference run	WRF	Decreased SST (0.6˚C) for the whole domain
2	Equal SST and LST	WRF	Align both the SST and the LST (Land surface temperature). Both are set to the SST of the reference run.
3	Increased SST	WRF	Increased SST (3˚C) for the whole domain
4	Decreased SST	WRF	Decreased SST (3˚C) for the whole domain
5	Urbanization	WRF	Urbanize the entire coastal region (arcaded area in Figure 2.3)
6	De-urbanization	WRF	Ruralize the entire coastal region (arcaded area in Figure 2.3)

Table 2.4: Expected outcomes of the sensitivity experiments

SENSITIVITY EXPERIMENT	EXPECTED OUTCOME
REFERENCE RUN	-
EQUAL SST AND LST	With equal surface temperatures over land and sea, the temperature gradient induced wind is expected to be minimalized, creating a stable atmosphere with little turbulence that should create better conditions for the initiation of coastal fog. However, this would reduce a possible sea breeze circulation which is possibly needed to obtain coastal fog. Furthermore, land surface heat fluxes should decrease resulting in a colder air parcel which can hold less water vapor which diminishes the fog formation.
INCREASED SST	An increased SST decreases the temperature gradient between the moist air parcel and sea surface temperature, along with an increased dew point temperature. One would expect the fog cloud to be smaller and have a shorter lifetime.
DECREASED SST	A decreased SST increases the temperature gradient between the moist air parcel and the sea surface temperature, along with a decreased dew point temperature. A larger fog cloud with a longer lifetime would be expected.
URBANISATION	Urbanization of the coastal area should increase surface heat fluxes and therefore heat up the moist air parcel (more than in the reference run) that is advected seaward, allowing the air to hold more water vapour which should enhance the fog formation.
DE-URBANISATION	De-urbanization of the coastal area should decrease heat fluxes and thus have a smaller heating effect on the air parcel advected seaward than the reference run, resulting in an air parcel with less water vapor, diminishing the fog formation.

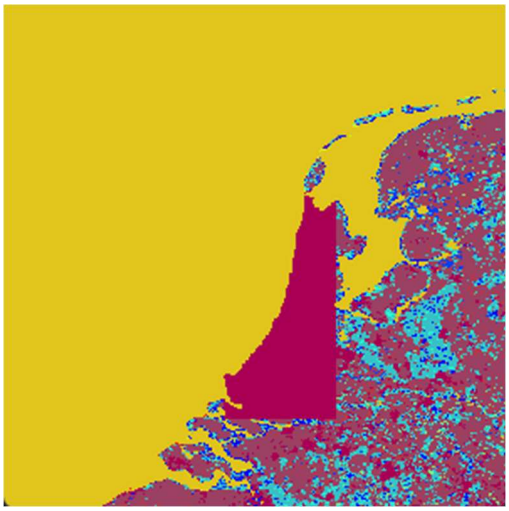

Figure 2.3: spatial representation of the area of which the land use was adjusted for sensitivity experiments 3 and 4.

2.5. Analysis

After validation of the reference run, the different sensitivity experiments are compared to the reference run to see the effect of the parameter adjustment in the model. A spatial analysis has been done to visualize the initiation and duration of the coastal fog. Changes in timing and density of the fog are two important components that need to be solved for the different sensitivity experiments. The most important variables that will be analysed with the goal to explain said changes are shown in Table 2.4.

Table 2.3: A description of the different variables that were analysed.

VARIABLE	UNIT	DESCRIPTION
Q_CLOUD	(gkg^{-1})	Q_cloud represents the specific humidity associated with cloud water. Spatial pictures of domain 2 including Q_cloud will be shown to visualize the shape, density and timing of the fog.
LWP	(gm^{-2}) or (mm)	LWP represents the liquid water path. It refers to the amount of liquid water that is present in a vertical column of air.
RH	(%)	RH represents the relative humidity, which is a crucial variable for the initiation of fog.
HFX	(Wm^{-2})	HFX represents the sensible heat flux. The difference between the total HFX over land and total HFX over sea will be compared.
WIND SPEED AND DIRECTION	(ms^{-1}) and (°)	The wind direction is important for the fog to reach the shoreline and the wind speed is an important factor that influences the duration and thus timing of the fog. Analysation of the windspeed is also important to capture circulations like the sea breeze circulation.

3 Results

This chapter will start with the results of the model validation, after which the results of the different experiments are illustrated stepwise.

3.1. Validation of WRF

Validation of the WRF model has been done by comparing the observations retrieved from the KNMI with the model results obtained by WRF for three meteorological weather stations shown in Figure 2.1. Euro platform, P11B and HoornA.

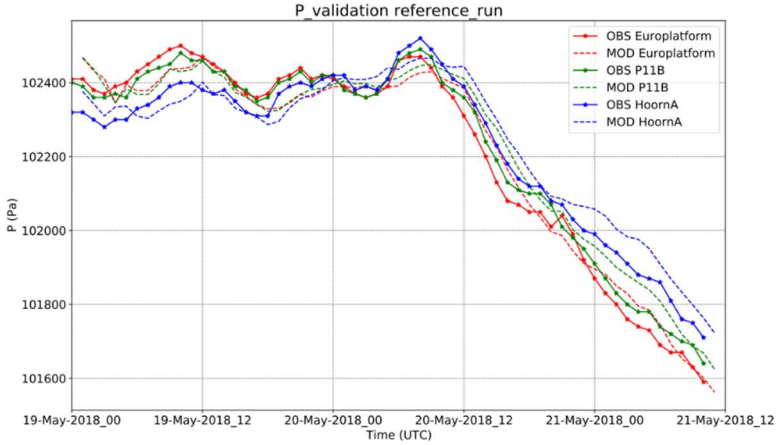

3.1a

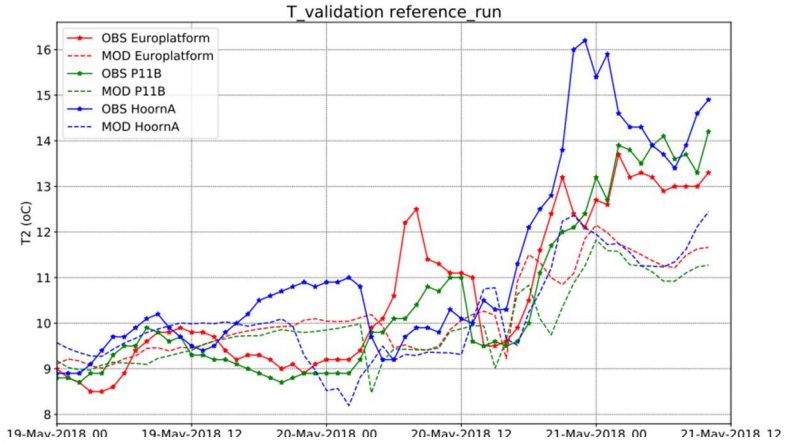

3.1b

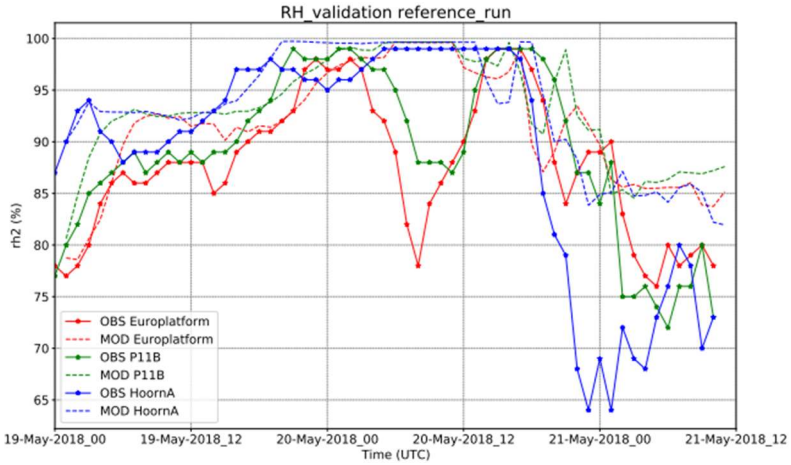

3.1c

Figure 3.1: Modelled and observed sea surface pressure (a), 2-meter temperature (b) and 2-meter relative humidity (c) at locations Euro platform, P11B and HoornA.

Table 3.1: Mean absolute error and root mean squared error for the temperature, sea surface pressure and relative humidity at Europlatform, P11B and HoornA

	STATION	P_SURFACE	T2	RH2
MEAN ABSOLUTE ERROR	**Euro platform**	31.5	0.93	5.03
	P11B	27.2	1.04	5.12
	HoornA	26.8	1.26	4.91
ROOT MEAN SQUARED ERROR	**Euro platform**	37.0	1.15	6.66
	P11B	31.6	1.30	6.50
	HoornA	32.2	1.70	7.36

The sea level pressure of all three measurement locations show similar results, as the same trend and approximately the similar values are shown over time. A mean absolute error (26.2 to 31.5) and a root mean squared error (31.6 tot 37.0) with both values around 0.03% of the variable's magnitude for all locations reaffirm this finding. This strengthens the validation of the synoptic situation simulation by WRF, because it is in agreeance with the observations. Both the 2-meter relative humidity (RH2) and the 2-meter temperature (T2) show larger differences between observed and modelled values than for the sea level pressure. These differences can be explained by timing and location of the fog which can create substantial local differences. The RH2 of 100% for the modelled data indicate the presence of fog for all three stations in the morning on the 20th of May. HoornA even shows an RH2 of 100% from 20:00 the evening before up until 13:00 on the 20th. Locations P11b and Euro platform show an RH2 of 100% from 05:00 until 11:00 and 06:00 until 11:00 respectively. Observations only indicate fog at HoornA from 05:00 until 16:00 and a temporary decline of the RH2 for P11B and Euro platform in the course of the morning. Simultaneously with the decrease in RH2 at Euro platform and P11B in the observations, the T2 rises, which can be directly related to the absence of fog. A small misplacement of the fog or different timing has a significant influence on the difference in RH2 and T2. Furthermore, during the last 12 hours, the simulation decreases in accuracy as the modelled T2 is on average about 3 degrees below the observed, the RH2 10 to 15 percent higher, and even the sea level pressure shows a larger deviation than the 48 hours before.

On the 20th of May 2018, the coastal fog was observed for a couple of hours starting at 10:00 (08:00 UTC). In Figure 3.4, spatial visualisations of both the modelled and observed coastal fog at 13:02 (11:02 UTC) and 15:10 (13:10 UTC) are shown respectively. The shape of the modelled fog cloud helps with explaining the large difference in the morning of the 20th, as the part of the cloud located between latitudes 52˚N and 53˚N and longitudes 2˚E and 3˚E advected over the meteorological stations P11B and Euro platform, which was not observed. However, when comparing both pictures in shape and timing, WRF seems to perform a satisfactory job at simulating the coastal fog case on the 20th of May 2018. Despite the described biases in the WRF model and taking into account the general difficulty for numerical models to capture sea fog, it can be decided to continue with the sensitivity experiments.

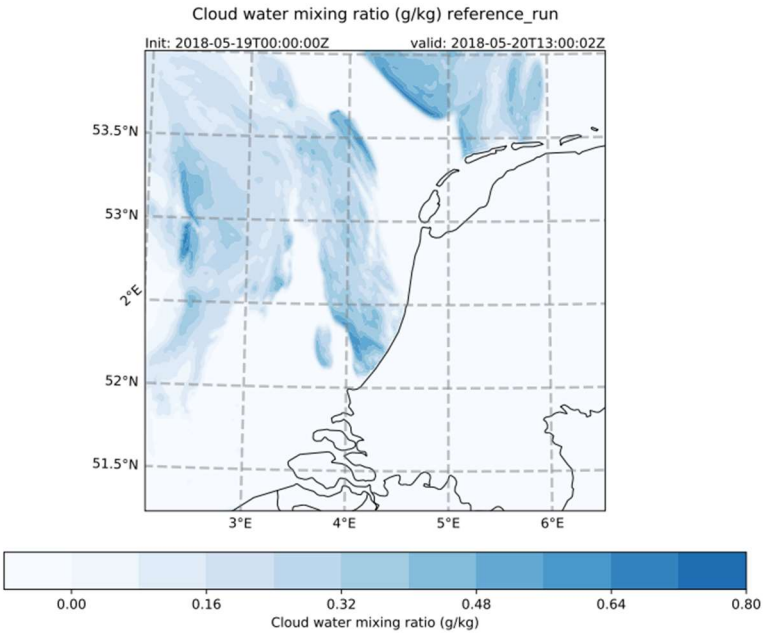

a: Modelled output of the cloud water mixing ratio (g/kg) at the surface on May 20th 2018 13:02 (UTC)

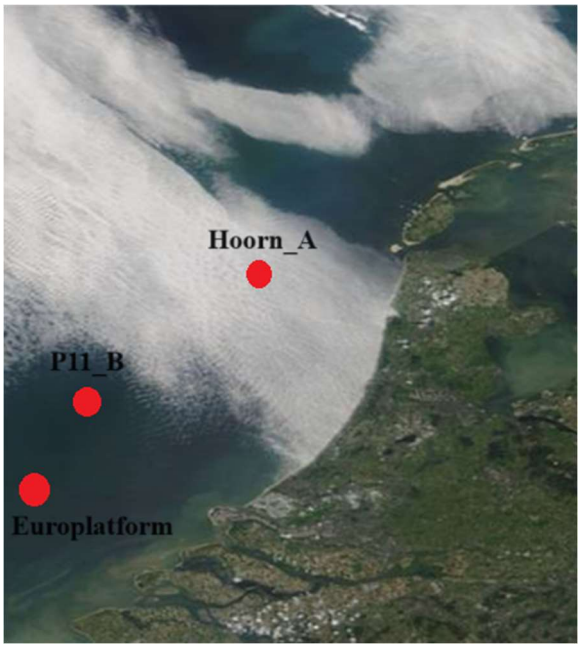

b: satellite image of the observed coastal fog on May 20th 2018 15:10 (UTC) on the North sea (KNMI, 2018)

Figure 3.2: Modelled (a) and observed (b) appearance of coastal fog

3.2. Sensitivity experiments

After validation of the reference run, multiple sensitivity experiments were performed and have been described in Table 2.3. To obtain these variables, the rectangle shown in Figure 3.5 is split by a diagonal similar to the shoreline of the coast, approximately between latitudes 52˚N , 53˚N and longitudes 4˚E, 5˚E. To obtain the total sensible heat flux (HFX) over land and over sea, the rectangle shown in Figure 3.5 is split by a diagonal similar to the shoreline of the coast, approximately between latitudes 52˚ , 53˚N and longitudes 4˚E, 5˚E. In Figure 3.9, the total HFX left of the diagonal (sea) is compared to the total HFX right of the diagonal (land), to use as a proxy to determine the strength of the sea breeze. Figure 3.10 contains a vertical transection of 1500 meters along the red line in Figure 3.6. Figure 3.10 spatially visualizes the liquid water path over the whole vertical column of the domain, which is expressed in meters. Above the mist layer, neither of the experiments simulated substantial clouds.

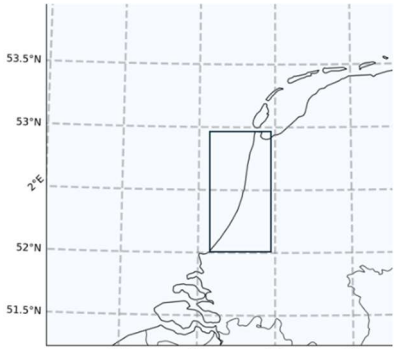

Figure 3.5: Representation of the analysed area in Figure 3.9

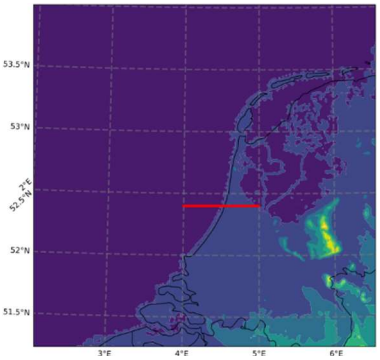

Figure 3.6: Representation of the location of the cross-section in Figure 3.10

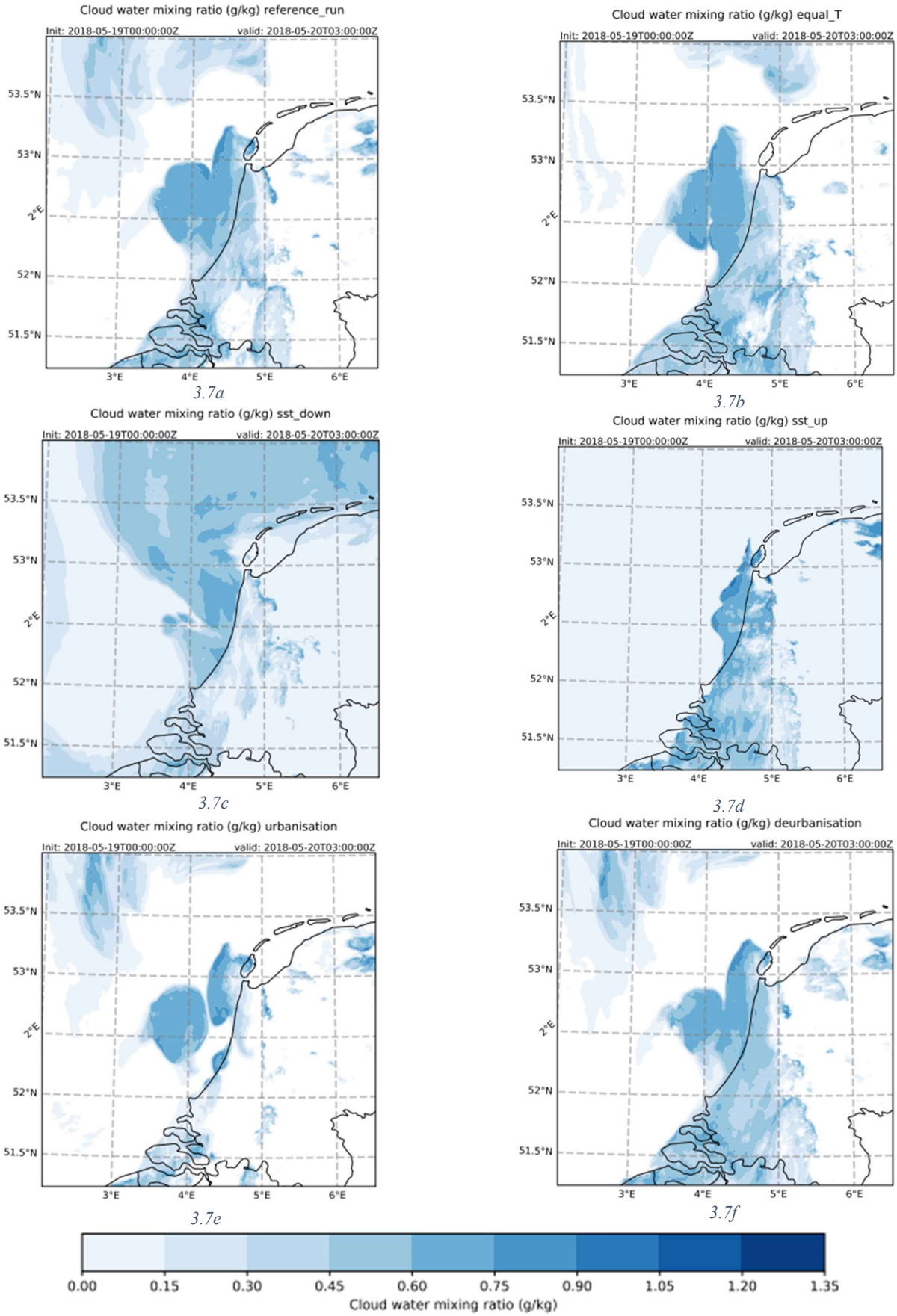

Figure 3.7: Modelled spatial distribution of liquid water concentration at model level 0 (0 meter above ground level) on the 20th of May 03:00 (UTC)

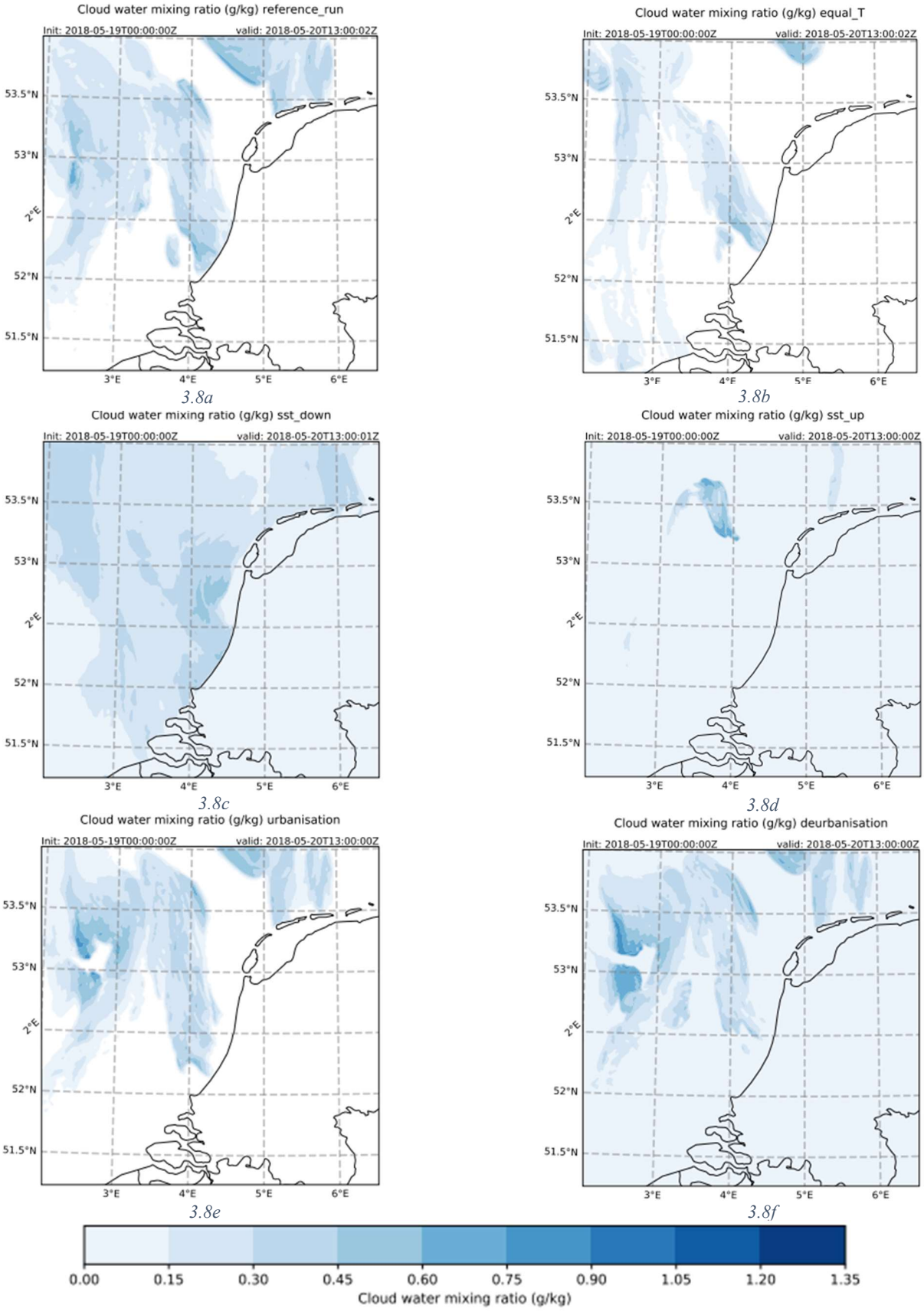

Figure 3.8: Modelled spatial distribution of liquid water concentration at model level 0 (0 meter above ground level) on the 20th of May 13:00 (UTC)

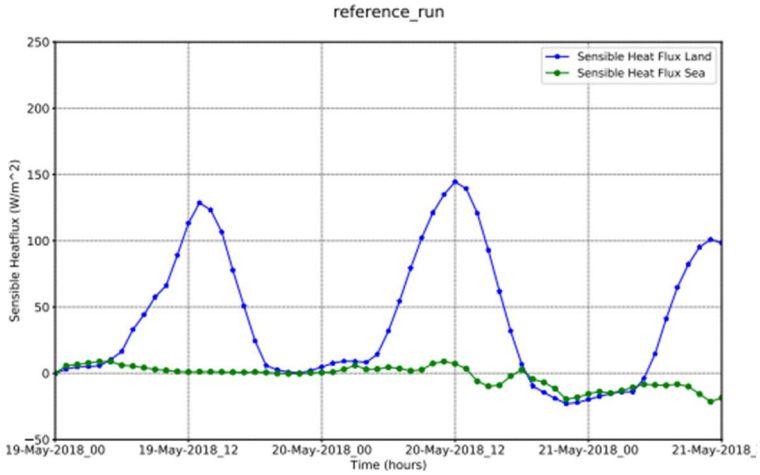

3.9a

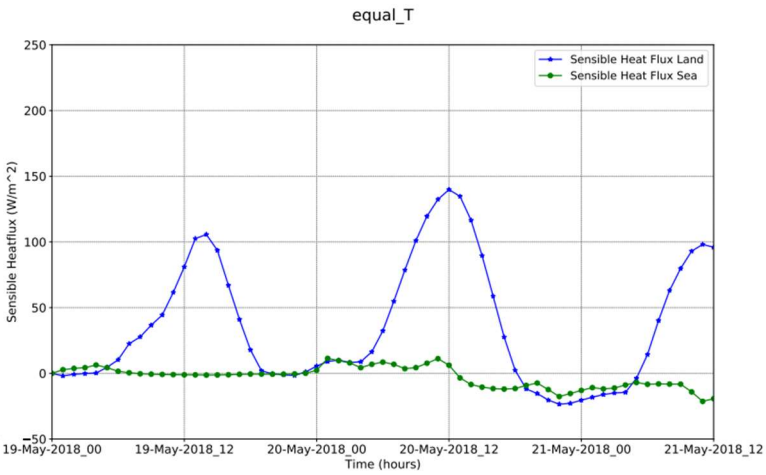

3.9b

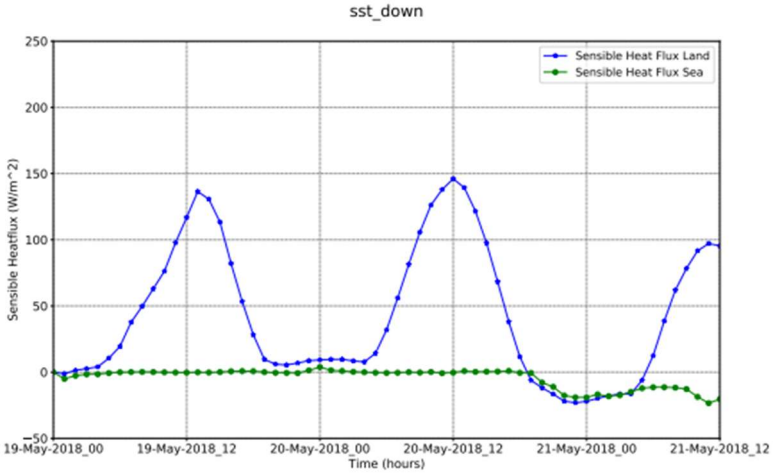

3.9c

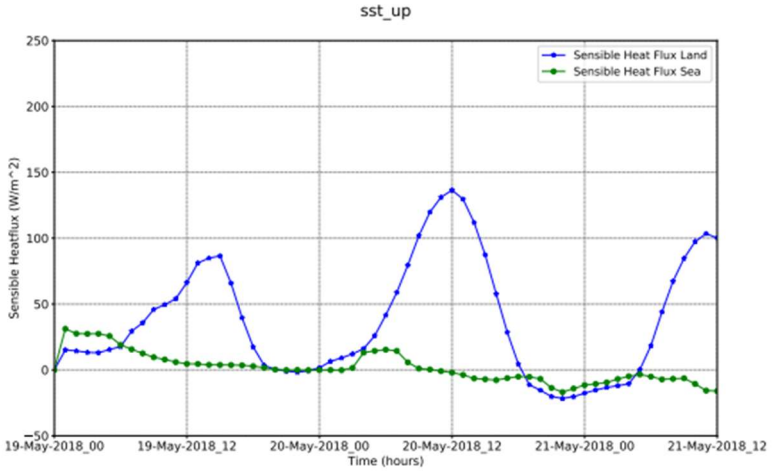

3.9d

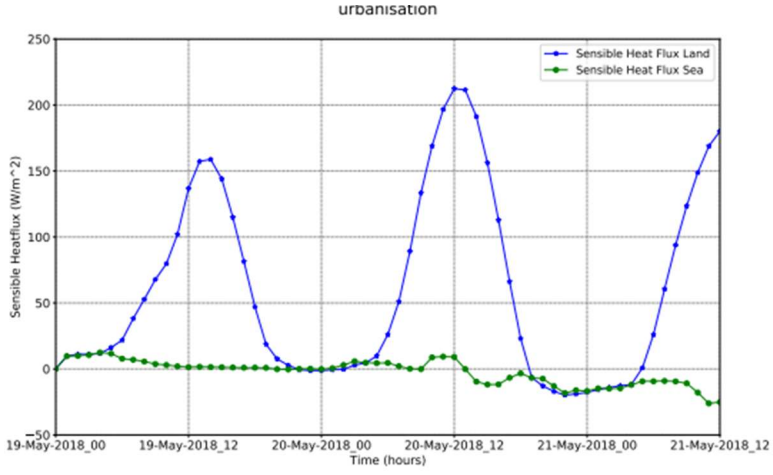

3.9e

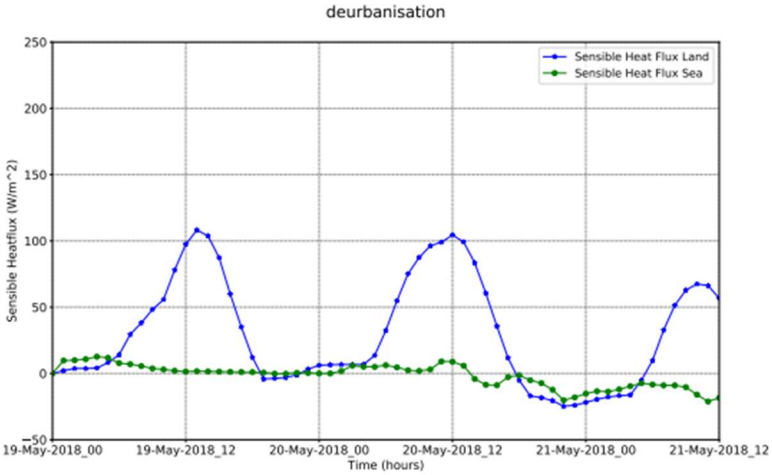

3.9f

Figure 3.9: Time series of the modelled sensible heat flux over land and sea for sensitivity experiments listed in table 2.3

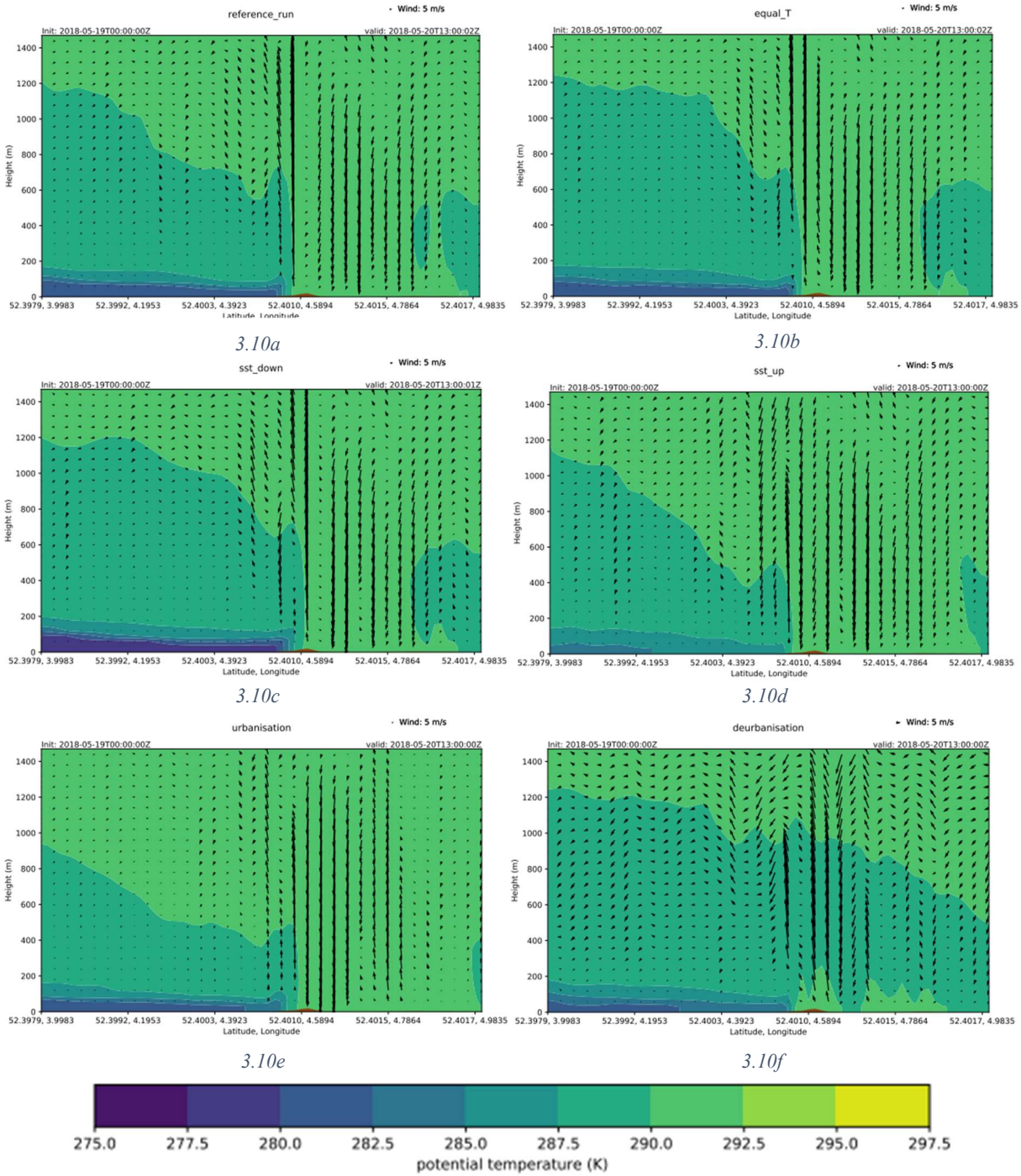

Figure 3.10: Transect of modelled field of wind direction and magnitude shown by the arrows and potential temperature represented by the background colours. The small orange hump at approximately longitude 4.6 represents the dune hills of the shoreline. This also helps with clarifying where the sea and the land are in these cross sections. The small arrow right above the transect represents 5ms^{-1} and gives a proper indication on the magnitude of the wind

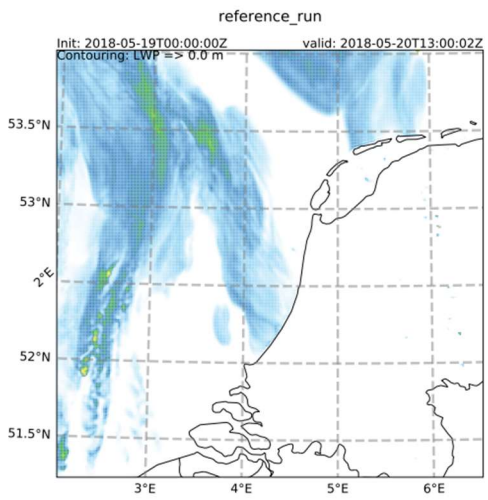

3.11a

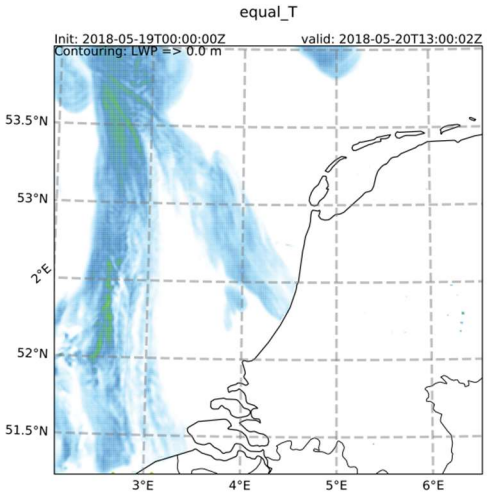

3.11b

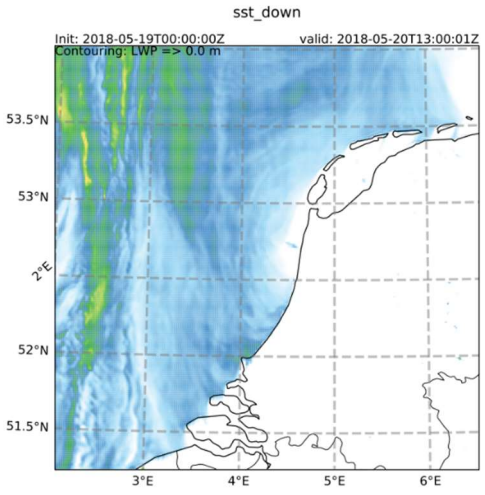

3.11c

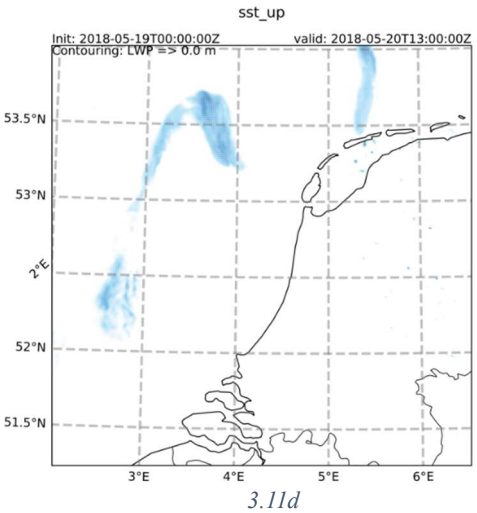

3.11d

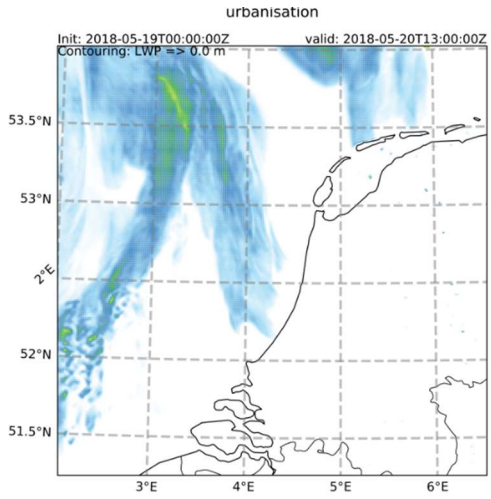

3.11e

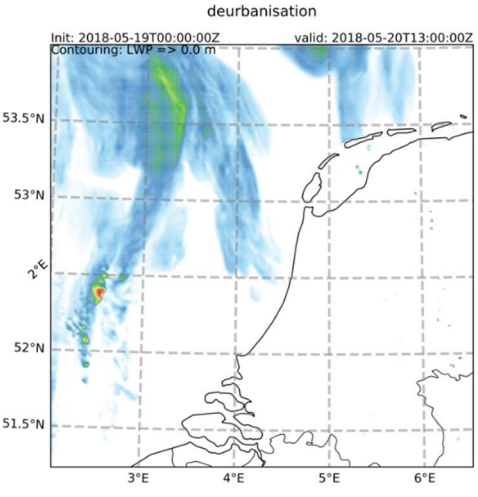

3.11f

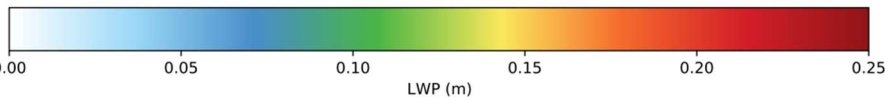

Figure 3.11: Modelled spatial distribution of liquid water path over the full vertical model column on the 20th of May 13:00 (UTC)

3.2.1. Reference run

In Figure 3.10a, the relatively low potential temperature in the lowest 100 meters near the sea surface mimics the cold pool that is in agreeance with the presence of fog. Figure 3.7a strengthens this finding as the fog reaches up to the coastline like the low potential temperature does. The transect shows near to windless conditions at the first couple hundred meters above the surface. There is only a very small westerly wind below 0.5 ms^{-1}. During the hours before the displayed Figures (at 13:00 UTC), the fog starts at sea and slowly expands towards the coastline. Both the cloud water mixing ratio (QCLOUD) and the potential temperature show this trend. After 13:00, both variables retreat seaward again. A sea breeze circulation (SBC) can be identified during the spin up of the simulation. The liquid water path (LWP) shows the presence of water land inwards where no fog occurs at the surface, indicating the formation of cumulus clouds, which can be associated with the SBC. The SBC weakens towards the appearance of coastal fog, after which the winds turns.

3.2.1. Equal Temperature

Experiment: All grid cells have an initial surface temperature of 283.17 K (10.02˚C), both SST and LST.

The equal temperature experiment has been conducted with the incentive to diminish the wind blowing between land and sea. Figure 3.10b exposes that the observed wind still follows the same patterns and the same magnitude as the wind in the reference run in Figure 3.10a. However, the easterly wind above is a bit weaker for the equal temperature experiment, indicating that the experiment results in a slightly diminished wind but not as extensive as hypothesized. The effect of the decreased land surface temperature can be visualized in Figure 3.9a and b, where the HFX reaches up to a max of 110 W/m^2 for the equal T experiment compared to 138 W/m^2 for the reference run during the 19th. On the 20th however, the max HFX is nearly equal again around 140 W/m^2. This is in accordance with the modelled land surface temperature which has recovered to similar temperatures as in the reference run. Noteworthy is, that still a smaller fog cloud seems to be formed as can be seen in Figure 3.7a and b, which is in line with the smaller liquid water path (LWP) shown in Figure 3.11b. Thus, the decreased initial land surface temperature has a reducing effect on the fog and cloud formation.

3.2.2. SST up and SST down

Experiment: All grid cells representing sea surface got a SST of 3˚C higher than the reference run for SST up and 3˚C lower than the reference run for SST down.

As has been hypothesized, a higher SST indeed results in less fog formation and a lower SST results in more fog formation as can be seen in figure 3.8c and 3.8d. This can be closely related to the decreased/increased temperature gradient between the warm moist air parcel and the cold sea surface that come into contact. For the lower SST experiment, the coastal fog expands substantially and touches upon the whole coastline of the Netherlands. Coastal fog is modelled during the whole night starting in the North of the Netherlands and expanding over the whole coastline during the morning, after which it slowly starts to dissipate after 13:00 and is completely cut off from the coast around 18:00.

The higher SST experiment mostly models fog over land during the night, which quickly dissipates in the morning when solar radiation has a heating effect on the surface. During the day almost all the fog is dissipated and a small plume of fog more than 50 km off coast is left at 13:00, so no occurrence of coastal fog. The potential temperature in Figure 3.10c and d and the LWP in Figure 3.11c and d confirm the presence of both the large fog cloud and the small fog cloud for lower SST and higher SST respectively. The cloud water mixing ratio of the fog in the lower SST experiment is not higher than for the reference run. Hence, the fog is formed faster but not denser.

Another notable difference between the SST-up and SST-down experiment is the height at which condensation occurs. The lower SST causes condensation to occur at the sea surface and the fog reaches up to a height of a 100 meters. With SST-up, condensation above marine area starts at 1500 meter, forming clouds far above the surface. The higher SST enhances evaporation which increases the

moisture content in the air. This causes an increasing formation of cumulus clouds over land enhanced by the SBC during the spin up time. Especially during the night towards the 20th of May, as the temperature gradient is now reversed with an SST that is about 2˚C higher than the LST. The LWP above land reaches up to 0.15 meter for SST-up compared to 0.05 meter for SST-down, a factor of three times the magnitude. The SST-down scenario shows a significantly higher LWP above the sea, reaching up to 0.5 meter, compared to 0.3 meter for SST-up.

An SBC cannot be identified in either of the SST experiments. However, the SST down experiment results in windless conditions at the surface, while the reference run simulates an eastern wind of maximal 2 ms^{-1} and the SST up experiment simulates eastern wind with wind speeds up to 3 ms^{-1}. So there is no SBC, however, the increased temperature gradient exerts a counterforce against the eastern wind, profitable for the fog maintenance.

3.2.4. Urbanisation and De-urbanisation

Experiment: The whole coastal area of the Netherlands (Figure 2.3) has been selected and changed to land use urban/rural(grassland/natural vegetation mosaic).

In this diptych of experiments, we anticipate that urbanization will enhance the fog formation, while de-urbanization will exert an adverse effect on the fog formation. Because cities are warmer than a countryside, resulting in a higher HFX and thus a potential promotion of the sea breeze circulation. Results show that urbanization and de-urbanization conduct an extension and a reduction of the dimension of the fog cloud respectively. Both experiments maintain the approximate shape of the reference run, as can be seen in Figure 3.8e and 3.8f as well as for the liquid water path which indicates the same. Urbanization results in a cloud diameter of approximately 47 km compared to approximately 37 km for the reference run. The diameter of the fog cloud after deurbanization is about 20 km. Even though the fog cloud is extended after urbanization, the cloud does not reach the coastline, which makes it no case of coastal fog. So fog formation is enhanced, but not all up to the coastline. This might be linked to the urban circulation that can be seen in Figure 3.10e immediately right of the coastline. Strong vertical up and down drafts that collectively form a local circulation above the urban land. This circulation is the most dominant wind pattern in the urbanization experiment and it includes downward vertical movement above the coastline of over 30 ms^{-1}, whereas the reference run shows a downward vertical wind speed of maximum 10 ms^{-1}.

3.2.5. Correlation

Previous sections in this chapter have shown that both the temperature gradient and the fraction of urbanization play an important role in the initiation and maintenance of coastal fog. To contribute to a better forecast of coastal fog, for instance a correlation between both factors might be produced, where a certain fraction of urbanization of the coastal area would be linked to a threshold land-sea temperature gradient for which coastal fog is likely to form.

4 Discussion

This chapter will include a discussion on the validity of the WRF model, the formation and maintenance of the fog, limitations and further research directions.

4.1. Validity of Results

Validating model simulations using WRF is crucial for ensuring the reliability of the sensitivity experiments outcomes. It is important to recognize that while the WRF model aims to replicate the coastal fog event on the 20th of May 2018, it relies on mathematical calculations, assumptions and parameterizations. Due to the inherently turbulent nature of the atmosphere, perfect replication is not realistic. However, despite this disclaimer, WRF produces a coastal fog simulation that resembles both shape and timing of the observed case study, as can be seen in Figure 3.4.

Upon closer examination of the results, notable differences between modelled and observed fog can be identified. Particularly, significant differences in temperature and relative humidity are observed at two of the three observational points during the morning preceding the coastal fog event. These deviations can be attributed to simulated fog that did not occur in reality. These findings are in line with Lee et al. (2021), who discovered WRF to properly simulate fog spatially while still having some local discrepancies. Lee et al. (2021) employed 51 vertical eta levels opposed to 44 levels for this case study, with similarly most of the levels close to the surface. Furthermore, they used 4 domains with increasing spatial resolution up to 3km^2 and 1km^2, identical to the spatial resolution I used in my two domains. He also used different boundary layers (YSU) and microphysics (WDM6) parameterization schemes, compared to this case where MYNN and Lin were used respectively.

4.2. Formation of Coastal Fog

This report examines multiple factors influencing coastal fog initiation, including sea surface temperature (SST) and its gradient relative to the land surface temperature (LST), atmospheric humidity content, wind conditions and stability of the atmosphere, all of which are interconnected. The consensus derived from this report regarding these factors is that the initiation of fog is enhanced by a higher temperature gradient between SST and LST, combined with a high atmospheric stability and a moisture content reaching up to saturation. This is in line with previous research on the formation of fog over marine areas (Fernando et al., 2021; Lee et al., 2021). The occurrence of coastal fog as described in Chapter 1 (the fog reaches up to the shore where it dissipates landward) proves to be more complex as not all results are in line with the expected outcomes. Multiple conditions are contradictory regarding enhancement of initiation of coastal fog.

A higher land surface temperature created with the urbanization experiment increases the peak sensible heat flux (HFX) with 70 Wm^{-2} over the terrestrial coastal area which results in a warmer air parcel that can hold more moisture, favouring the formation of fog when this warm moist air parcel is advected over the cold sea surface. Simultaneously, an increased HFX results in an increased turbulence in the air parcel, which manifested as a circulation above the urban land in the urbanization experiment. This does not have an effect on the formation of fog over the marine area. But once the fog moves landwards, it dissipates before reaching the shoreline as the turbulence above the coastal area causes relatively warmer terrestrial air to be mixed with marine air. The temperature gradient proves to have a larger impact on expanding the extent of the fog, than the turbulence near the coast has on the dissipation of the fog. The de-urbanization experiment supports this finding as the result shows a cloud reaching less far towards the shoreline while the experiment has a smaller land-sea temperature gradient and shows less turbulence over land near the shoreline. No research has been found that examines the influence of (de-)urbanization of a coastal area on the formation or lifetime of coastal fog, so there is no material for comparison of the results.

There is no clear answer on the question if coastal fog could occur without a sea breeze circulation (SBC) because the attempt to diminish the circulation did not go as planned. However, results of the other sensitivity experiments give some insights on the effect of the SBC on coastal fog. The SST-down experiment revealed that a larger temperature gradient amplifies a counterforce against the synoptical eastern wind in this case, which is in this instance coincided with a longer lifetime and a larger spatial extent of the coastal fog. Jin et al., (2022), who researched the influence of SBC on sea fog over the Yellow Sea in China, found that an SBC acts as an inhibitor that reduces sea fog formation. This finding is in disagreement with this case study and the previous interpretations described by Floor (2013). It must however be taken into account that Jin et al., researched sea fog as opposed to coastal fog. Furthermore, the Yellow Sea at the coast of China and the North Sea at the coast of The Netherlands provide, although both in a temperate maritime climate, two very different sets of conditions, making the comparison biased.

4.3 Limitations

Compared to multiple other studies who use up to 100 vertical eta levels (Jin et al., 2022; Lee et al., 2021; Fernando et al., 2021), the 44 vertical levels used in my experiments might fail to capture the details of critical processes like advection and turbulence. The amount of vertical levels was chosen in order to keep the simulation time and costs to a minimum.

An important factor that has not been experimented with or discussed in this study is the impact of cloud condensation nuclei (CCN). These are very small particles that enhance the droplet formation and are thus at the basis of cloud formation (Hudson, 1993). Urban areas have a significant impact on the amount of CCN (Vo et al., 2023), which is an important contributor to the formation of coastal fog. With a higher CCN concentration over sea it would be expected that fog formation is enhanced due to an increased droplet formation (Reutter et al., 2009).

Parameterization schemes, consisting of mathematical calculations or algorithms help WRF with processing variables. Although this helps with simplifying calculations and thus speeding up the simulation, it brings along some limitations as well. Some parameterization schemes are not compatible with certain settings in WRF. For this study, the MYNN planetary boundary layer parameterization scheme was used because this scheme proved to perform best in simulating fog. However, MYNN is not compatible with the urban scheme which activates a more detailed algorithm for the urban area. Therefore the urban scheme could not be used in this research. An even more turbulent air movement could be the result of a simulation for which the urban scheme was indeed activated.

This study was solely based on one case of coastal fog. A better understanding of its formation and maintenance can be obtained when multiple cases with different synoptical situations are analysed.

4.5. Future Research Directions

Further investigations are needed to deepen our understanding of the complex interconnection between urbanization, land-sea temperature gradients and the formation of coastal fog. As discussed, a correlation might be identified between the fraction of urban area and the magnitude of the land-sea temperature gradient to find which combination of these factors enhances or diminishes the formation of coastal fog. A threshold might be identified for which marine fog transitions into coastal fog.

This research indicates subtly that coastal fog can occur without the presence of SBC. However, the influence of SBC on the formation of coastal fog can be investigated further. Especially the difference between daytime and nighttime, to identify the intercorrelation between both phenomena. An option for a sensitivity analysis on this matter could be to inactivate the Coriolis parameter, as an attempt to diminish wind patterns.

5 Conclusion

In summary, this study aimed to address two key research questions. Firstly, it was tried to investigate the mechanism through which coastal fog formation could occur in the absence of sea breeze circulation. Secondly, it was sought to identify the meteorological variables and geographical characteristics that play a crucial role in initiating coastal fog. To achieve these objects, a series of sensitivity experiments where performed with WRF, including an increased/decreased sea surface temperature and an increased/decreased coastal urban area.

In conclusion, the dynamics of coastal fog formation are influenced by various factors, in which the land-sea temperature gradient plays a crucial role. A higher gradient, with relatively high temperatures over land and relatively low temperatures over sea, tends to enhance both the initiation and duration of coastal fog. Additionally, the proximity of urban areas to the coast can amplify the formation of marine fog while obstructing the transition to coastal fog due to turbulence near the shoreline that induces mixing of warm and cold air before the fog reaches the shoreline.

The question whether coastal fog can appear without an SBC remains partly unanswered due to an unexpected unfolding of the equal temperature experiment. Nevertheless, the other experiments provided insights to answer this question. The results argue that coastal fog should be able to develop independently of an SBC, although the presence of an SBC can intensify the fog formation. Notable, a stronger land-sea temperature gradient appears to induce an SBC, which could explain the frequently simultaneous occurrence of coastal fog and SBC. What we know for sure is that sea breeze circulation and coastal fog are closely related and SBC effects coastal fog, leaving us with speculation and further needed research on what this effect is exactly.

However, gaps in the understanding of coastal fog still exist, inducing the need of further investigation. Specifically, future research should focus on the understanding of the correlation between urban areas and land-sea temperature gradient with respect to coastal fog formation, as well as the interdependence of coastal fog on SBC. Furthermore, the influence of CCN should be taken into account in further investigations. Inactivating the Coriolis parameter could be a promising experiment to find the interconnection between coastal fog and sea breeze circulation. By expanding our knowledge in these areas, we can improve our ability to forecast and mitigate the impacts of coastal fog, hence providing safety in coastal regions.

Acknowledgements

I would like to express my thanks to my supervisor, Gert-Jan Steeneveld, for his guidance and support throughout the entirety of this thesis, which has not always been easy for me. His expertise and insights have been important in shaping the direction of this thesis. Gert-Jan also managed to provide me the right direction in times when I got lost, which helped me to stay motivated.

I would also like to thank Sjoerd Barten, member of the MAQ department, who helped me with lots of problems that occurred with High Performance Computer Anunna, or errors occurring in my Python scripts. I wouldn't have been able to finish this thesis without his help.

Special thanks Hannah who always believed in me when I needed someone to do so, not to forget that she also provided me feedback and a spelling check in the end.

Last but not least, I am thankful for all the students in the thesis ring from whom I received insightful feedback that improved the quality of my work. Special thanks to Dennis Schoonhoven, Rick Neulen, Ment Reeze, Federico Battistig, Luce Creman, Manou Spoor, Marin Schadee and Anastasia Ionas, with whom I spent most of the time in the thesis ring with. Also thanks to the supervisors of the group, Menno Veerman and Remco de Kok.

References

1. Angell, J. K., & Pack, D. H. (1965). A study of the sea breeze at Atlantic City, New Jersey using tetroons as Lagrangian tracers. *Monthly Weather Review*, *93*(8), 475-493.
2. Camberlin, P., & Planchon, O. (1997). Coastal precipitation regimes in Kenya. *Geografiska Annaler: Series A, Physical Geography*, *79*(1-2), 109-119.
3. Coping With Sudden Fog. (2019). https://www.boatus.com. https://www.boatus.com/expert-advice/expert-advice-archive/2019/april/coping-with-sudden-fog
4. Dorman, C. E., Grachev, A. A., Gultepe, I., & Fernando, H. J. (2021). Toward improving coastal-fog prediction (C-FOG). Boundary-Layer Meteorology, 1-4.
5. Eckart, C. (2013). Hydrodynamics of oceans and atmospheres. Elsevier.
6. Fernando, H. J., Gultepe, I., Dorman, C., Pardyjak, E., Wang, Q., Hoch, S. W., ... & Wauer, B. (2021). C-FOG: life of coastal fog. Bulletin of the American Meteorological Society, 102(2), E244-E272.
7. Floor, K. (2013). Zeevlam zonder zeewind. Meteorologica, 1(22). 13-15.
8. Gultepe, I., Heymsfield, A. J., Fernando, H. J. S., Pardyjak, E., Dorman, C. E., Wang, Q., ... & Wang, S. (2021). A review of coastal fog microphysics during C-FOG. Boundary-Layer Meteorology, 181, 227-265.
9. Hong, S. Y. (2010). A new stable boundary-layer mixing scheme and its impact on the simulated East Asian summer monsoon. Quarterly Journal of the Royal Meteorological Society, 136(651), 1481-1496.
10. Hoofdstuk 7. Zicht, mist en dauw. (z.d.). https://www.keesfloor.nl/weerkunde/7zicht/7zicht.htm
11. Hudson, J. G. (1993). Cloud condensation nuclei. Journal of Applied Meteorology and Climatology, 32(4), 596-607.
12. Izett, J. G., van de Wiel, B. J., Baas, P., & Bosveld, F. C. (2018). Understanding and reducing false alarms in observational fog prediction. Boundary-layer meteorology, 169, 347-372.
13. Jin, G., Gao, S., Shi, H., Lu, X., Yang, Y., & Zheng, Q. (2022). Impacts of sea–land breeze circulation on the formation and development of Coastal Sea Fog along the Shandong Peninsula: a case study. Atmosphere, 13(2), 165.
14. Kain, J. S. (2004). The Kain–Fritsch convective parameterization: an update. Journal of applied meteorology, 43(1), 170-181.
15. KNMI. (12 june 2018). Zeevlam aan het strand. Retrieved from https://www.knmi.nl/over-het-knmi/nieuws/zeevlam-aan-het-strand
16. Lee, E., Kim, J. H., Heo, K. Y., & Cho, Y. K. (2021). Advection fog over the eastern Yellow Sea: WRF simulation and its verification by satellite and in situ observations. *Remote Sensing*, *13*(8), 1480.
17. Lin, Y. L., Farley, R. D., & Orville, H. D. (1983). Bulk parameterization of the snow field in a cloud model. Journal of Applied Meteorology and climatology, 22(6), 1065-1092.
18. Masselink, G. (1998). The effect of sea breeze on beach morphology, surf zone hydrodynamics and sediment resuspension. *Marine Geology*, *146*(1-4), 115-135.
19. Miller, S. T. K., Keim, B. D., Talbot, R. W., & Mao, H. (2003). Sea breeze: Structure, forecasting, and impacts. *Reviews of geophysics*, *41*(3).
20. Myers, J. N. (1968). Fog. *Scientific American*, *219*(6), 74-83.
21. Nakanishi, M. (2000). Large-eddy simulation of radiation fog. *Boundary-layer meteorology*, *94*, 461-493.
22. Nakanishi, M., & Niino, H. (2006). An improved Mellor–Yamada level-3 model: Its numerical stability and application to a regional prediction of advection fog. Boundary-Layer Meteorology, 119, 397-407.
23. Nakanishi, M., & Niino, H. (2009). Development of an improved turbulence closure model for the atmospheric boundary layer. Journal of the Meteorological Society of Japan. Ser. II, 87(5), 895-912.

24. Olson, J. B., Kenyon, J. S., Angevine, W., Brown, J. M., Pagowski, M., & Sušelj, K. (2019). A description of the MYNN-EDMF scheme and the coupling to other components in WRF–ARW.
25. Powers, J. G., Klemp, J. B., Skamarock, W. C., Davis, C. A., Dudhia, J., Gill, D. O., ... & Duda, M. G. (2017). The weather research and forecasting model: Overview, system efforts, and future directions. Bulletin of the American Meteorological Society, 98(8), 1717-1737.
26. Reutter, P., Su, H., Trentmann, J., Simmel, M., Rose, D., Gunthe, S. S., ... & Pöschl, U. (2009). Aerosol-and updraft-limited regimes of cloud droplet formation: influence of particle number, size and hygroscopicity on the activation of cloud condensation nuclei (CCN). Atmospheric Chemistry and Physics, 9(18), 7067-7080.
27. Roach, W. T., Brown, R., Caughey, S. J., Garland, J. A., & Readings, C. J. (1976). The physics of radiation fog: I–a field study. Quarterly Journal of the Royal Meteorological Society, 102(432), 313-333.
28. Silva Dias, M. A., & Jaschke Machado, A. (1997). The role of local circulations in summertime convective development and nocturnal fog in São Paulo, Brazil. *Boundary-Layer Meteorology*, *82*(1), 135-157.
29. Shao, N., Lu, C., Jia, X., Wang, Y., Li, Y., Yin, Y., ... & Lv, J. (2023). Self-enhanced aerosol–fog interactions in two successive radiation fog events in the Yangtze River Delta, China: A simulation study. Atmospheric Chemistry and Physics Discussions, 2023, 1-46.
30. Skamarock, W. C., Klemp, J. B., Dudhia, J., Gill, D. O., Liu, Z., Berner, J., . . . others (2019). A description of the advanced research wrf model version 4. National Center for Atmospheric Research: Boulder, CO, USA, 145 , 145.
31. Smirnova, T. G., Brown, J. M., Benjamin, S. G., & Kenyon, J. S. (2016). Modifications to the rapid update cycle land surface model (RUC LSM) available in the weather research and forecasting (WRF) model. Monthly weather review, 144(5), 1851-1865.
32. Srivastava, P. K., Han, D., Rico-Ramirez, M. A., O'Neill, P., Islam, T., Gupta, M., & Dai, Q. (2015). Performance evaluation of WRF-Noah Land surface model estimated soil moisture for hydrological application: Synergistic evaluation using SMOS retrieved soil moisture. Journal of Hydrology, 529, 200-212.
33. Steeneveld, G. J., Ronda, R. J., & Holtslag, A. A. M. (2015). The challenge of forecasting the onset and development of radiation fog using mesoscale atmospheric models. Boundary-Layer Meteorology, 154, 265-289.
34. Taylor, P. A., Chen, Z., Cheng, L., Afsharian, S., Weng, W., Isaac, G. A., ... & Chen, Y. (2021). Surface deposition of marine fog and its treatment in the WRF model. *Atmospheric Chemistry & Physics Discussions*.
35. Vo, T. T., Hu, L., Xue, L., Li, Q., & Chen, S. (2023). Urban effects on local cloud patterns. Proceedings of the National Academy of Sciences, 120(21), e2216765120.
36. Wolters, D., Homan, C., & Bessembinder, J. (2011). Ruimtelijke klimatologische verschillen binnen Nederland. Koninklijk Nederlands meteorologisch instituut, De Bilt.
37. Yang, Y., Hu, X. M., Gao, S., & Wang, Y. (2019). Sensitivity of WRF simulations with the YSU PBL scheme to the lowest model level height for a sea fog event over the Yellow Sea. Atmospheric Research, 215, 253-267.

6 Appendix

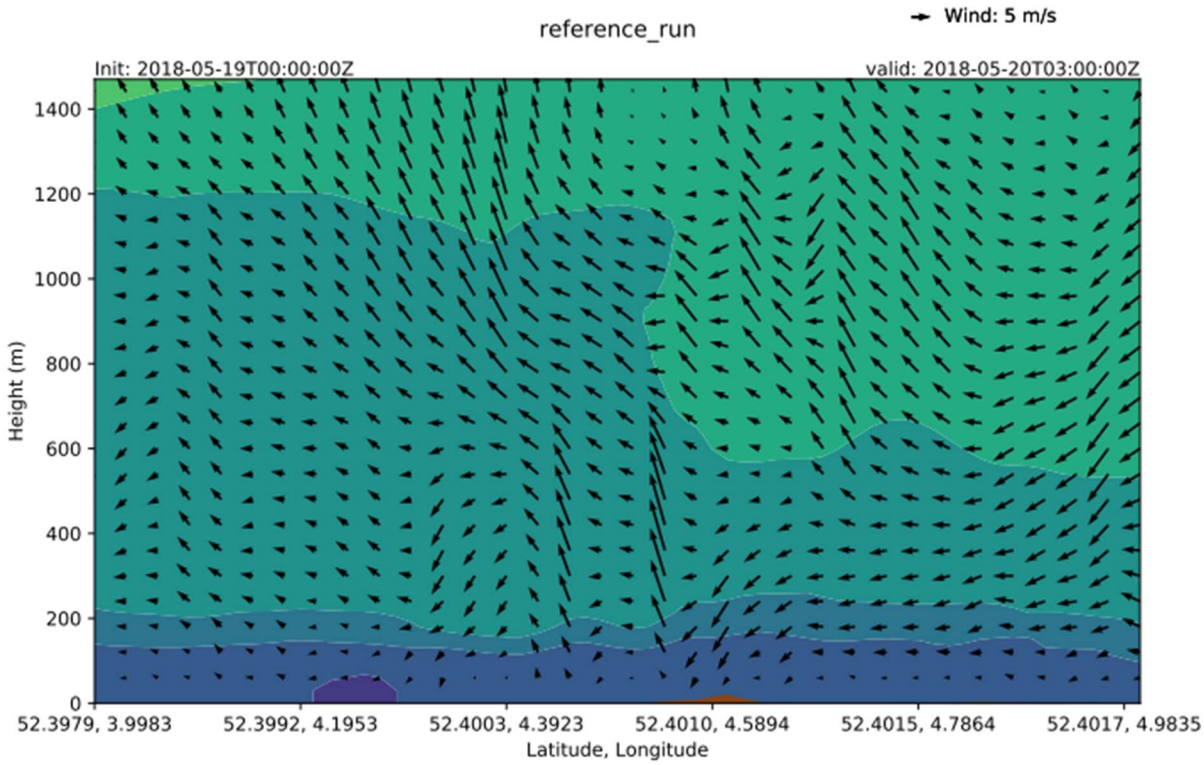

6.1a

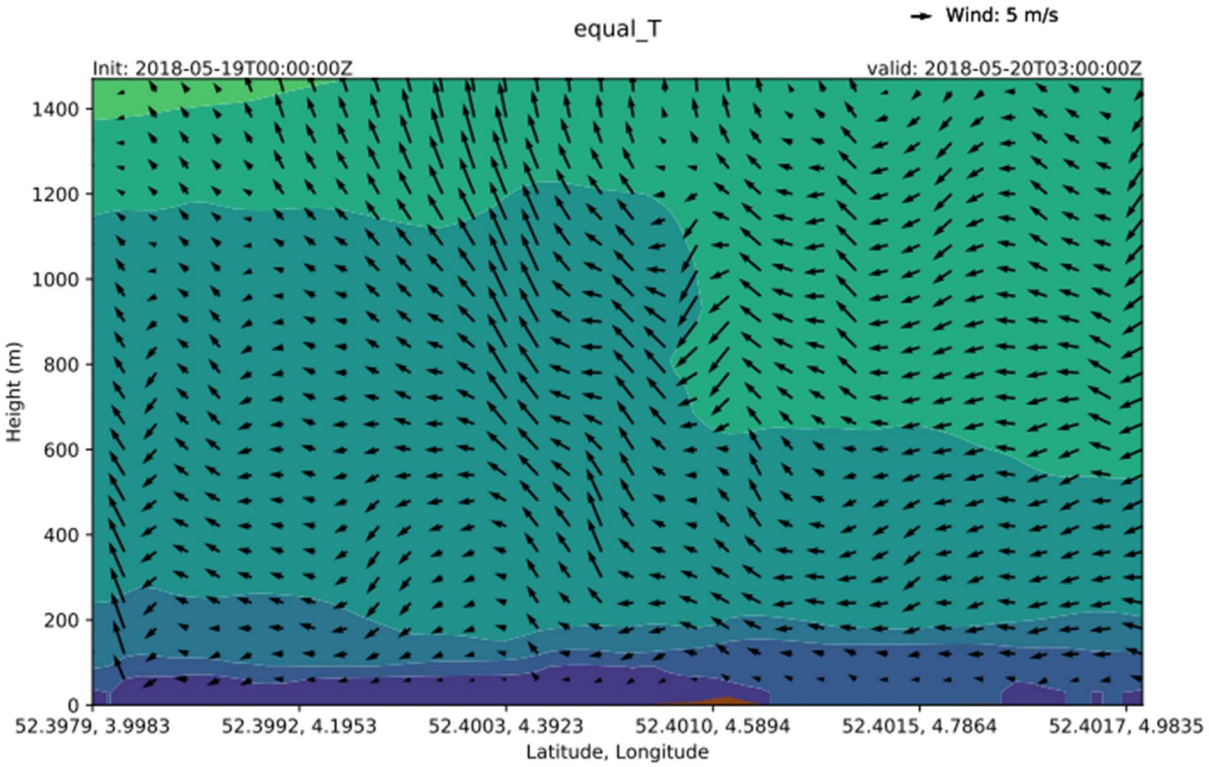

6.1b

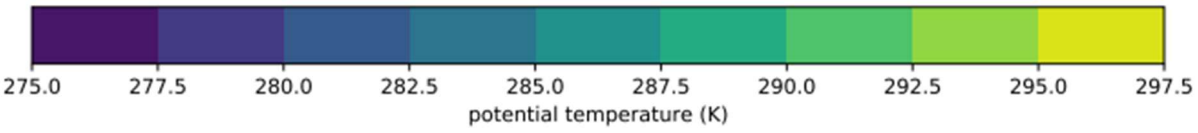

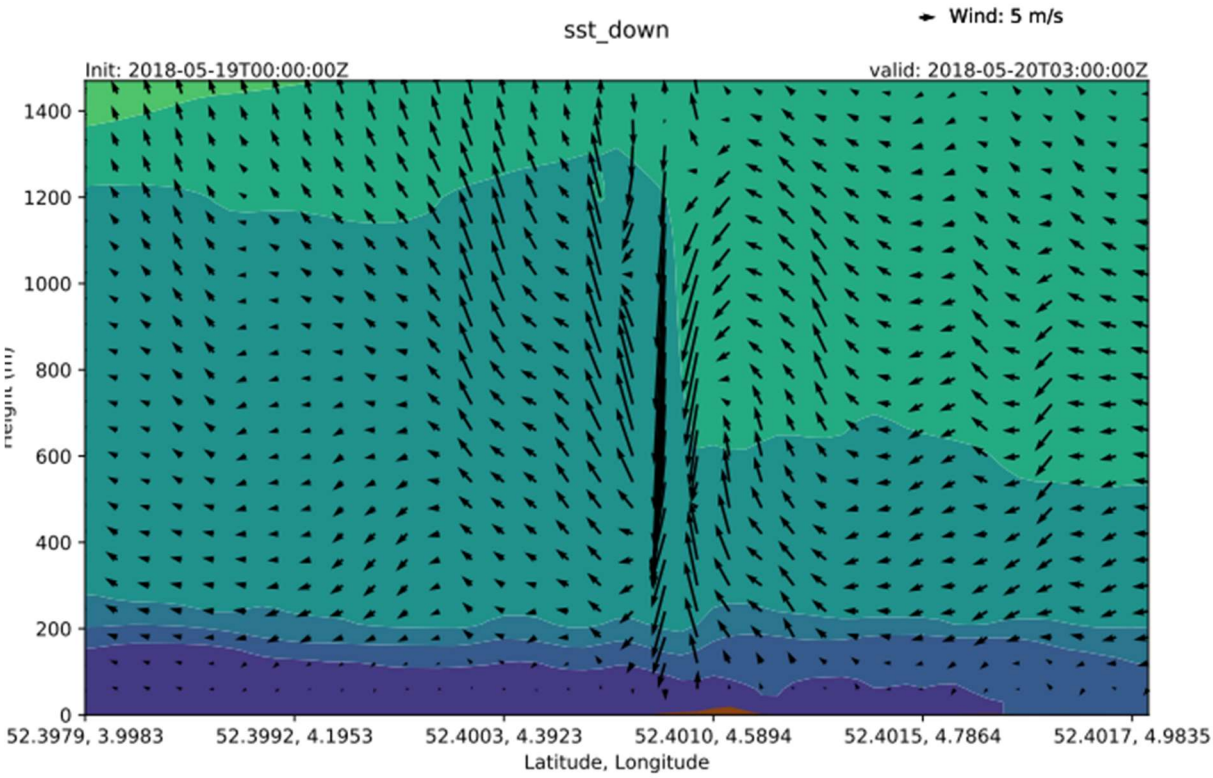
sst_down
Wind: 5 m/s
Init: 2018-05-19T00:00:00Z
valid: 2018-05-20T03:00:00Z
1400
1200
1000
800
600
400
200
0
52.3979, 3.9983
52.3992, 4.1953
52.4003, 4.3923
52.4010, 4.5894
52.4015, 4.7864
52.4017, 4.9835
Latitude, Longitude

6.1c

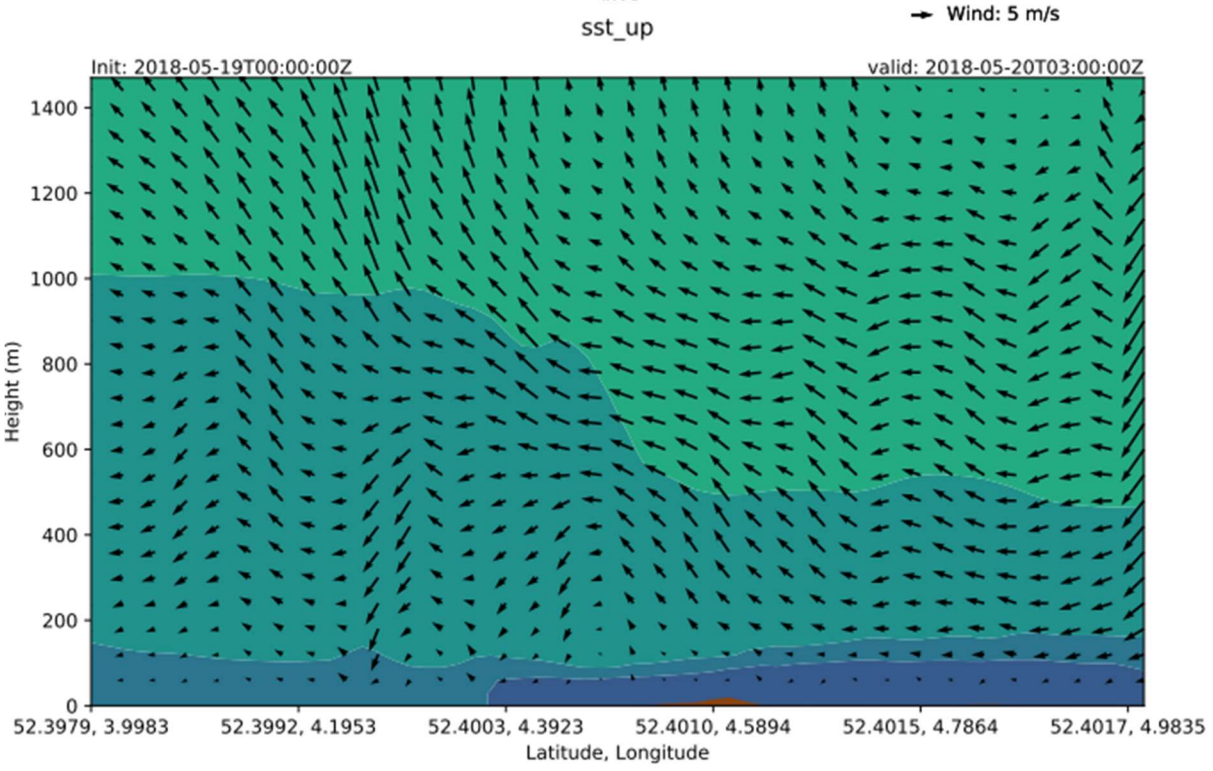
sst_up
Wind: 5 m/s
Init: 2018-05-19T00:00:00Z
valid: 2018-05-20T03:00:00Z
Height (m)
1400
1200
1000
800
600
400
200
0
52.3979, 3.9983
52.3992, 4.1953
52.4003, 4.3923
52.4010, 4.5894
52.4015, 4.7864
52.4017, 4.9835
Latitude, Longitude

6.1d

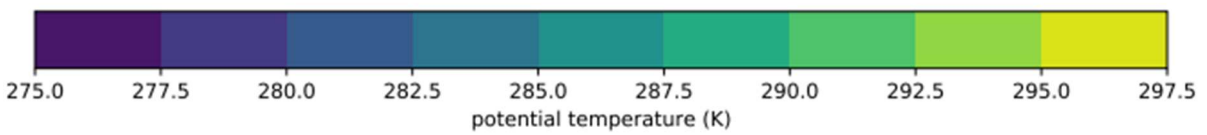
275.0
277.5
280.0
282.5
285.0
287.5
290.0
292.5
295.0
297.5
potential temperature (K)

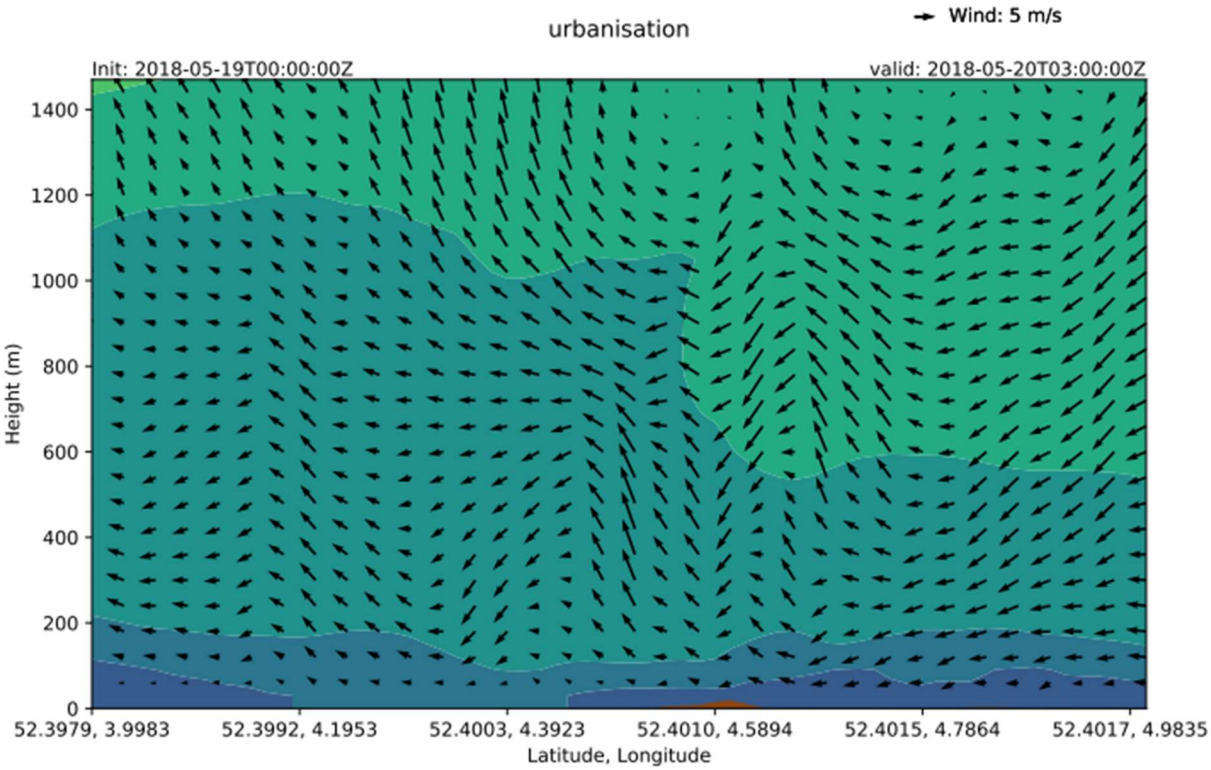

6.1e

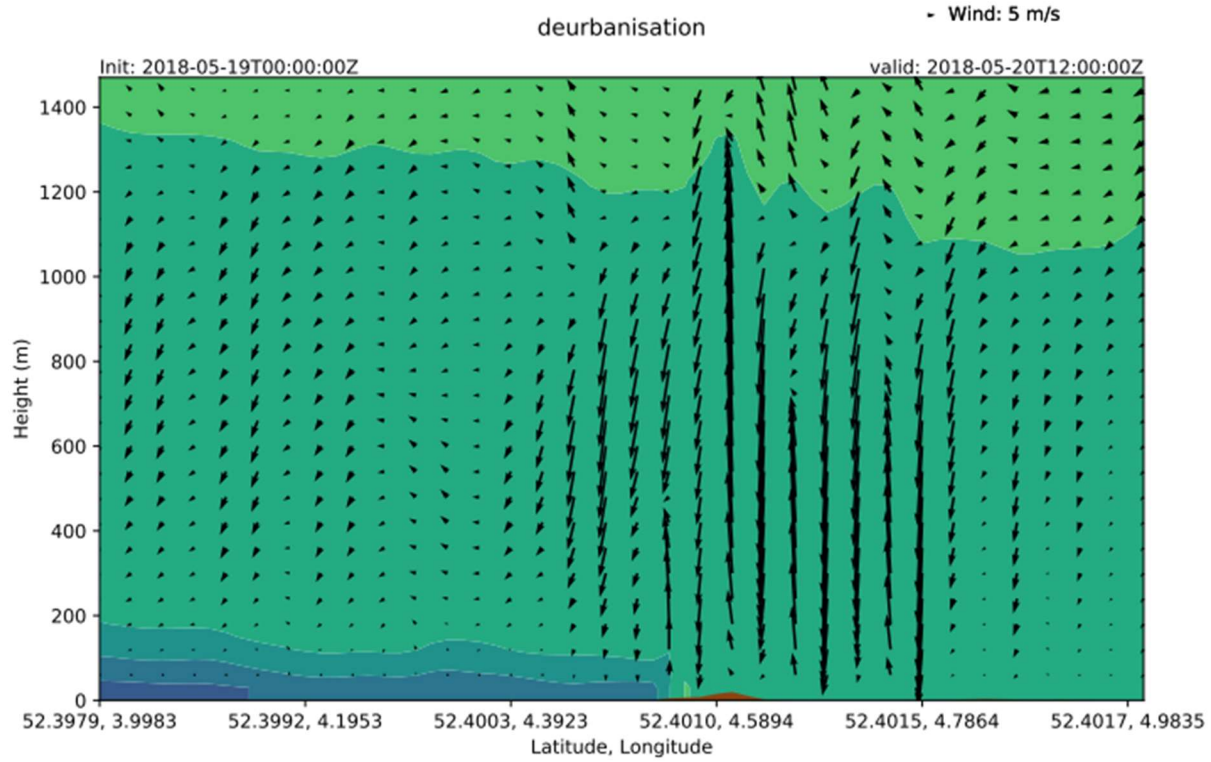

6.1f

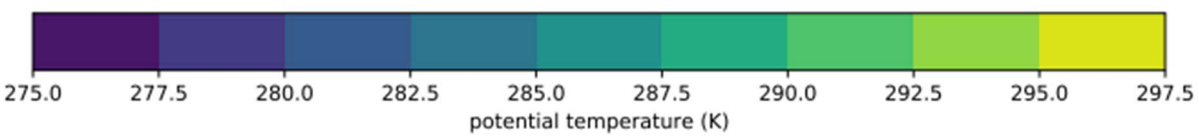

Figure 6.1: Transect of modelled field of wind direction and magnitude shown by the arrows and potential temperature represented by the background colours. The small orange hump at approximately longitude 4.6 represents the dune hills of the shoreline. This also helps with clarifying where the sea and the land are in these cross sections. The small arrow right above the transect represents 5ms^{-1} and gives a proper indication on the magnitude of the wind